INVESTIGATING TURBULENT CONVECTION IN A RECTANGULAR ENCLOSURE USING SHEAR STRESS TRANSPORT k-ω MODEL

BY

MUHORO JOHN NYAGA (B.Ed. Sc.)

REG. No: I56/CE/27833/2013

KENYATTA UNIVERSITY

A PROJECT SUBMITTED IN PARTIAL FULFILLMENT OF THE REQUIREMENTS FOR THE AWARD OF DEGREE OF MASTERS OF SCIENCE IN APPLIED MATHEMATICS IN THE SCHOOL OF PURE AND APPLIED SCIENCES

OF

KENYATTA UNIVERSITY

2020

DECLARATION

This project is my original work and has not been submitted in any other university in part or whole for a degree award.

Signature ……. Date……,

Muhoro John Nyaga

This project has been submitted with my approval as university supervisor

Signature ……. Date……,

Dr. Kennedy Otieno Awuor

Department of mathematics,

Kenyatta University.

DEDICATION

I wish to commit this project to my wife Joyce Wambui, daughter Amari Wanjiru and parents Grace Wanjiru and Joseph Muhoro for their devotion and inspiration.

I would also like to dedicate this project to Dr. K. O. Awuor for his guidance and encouragement to take this course.

ACKNOWLEDGEMENT

I wish to convey my heartfelt appreciation to my supervisor Dr. K. O. Awuor, who shepherded me through this work. This project would not have been successfully completed without his valuable words of encouragement, friendship support and inspiration.

I also acknowledge with much appreciation the crucial role of the staff of Mathematics department, Kenyatta University who diligently took us through the course work.

I would also like to thank Ntunene Girls staff especially Mr. Mwaniki and Mrs. Muturia, whose encouragement and motivation helped me to undertake this course.

To my course mates, especially Michael Gicheru, for constant discussions we had throughout the course.

I wish to acknowledge the moral support from my family who did not at any one-time hold any reservations to my undertaking this study. I sincerely thank them for believing in my capabilities and encouraging me untiringly especially in difficult circumstances during the period of my study.

Above all to God Almighty for His sufficient blessing and favor throughout my studies.

TABLE OF CONTENTS

LIST OF FIGURES

LIST OF TABLES

Nomenclature

Symbol	**Quantity**
μ	Dynamic viscosity
ε	Dissipation
ρ	Density
g	Acceleration due to gravity
C_p	Specific heat capacity
F_i	Body forces
V_t	Kinetic turbulent viscosity
$\vec{V}$	Velocity
A	Acceleration
p.d.e.	Partial differential equation
CFD	computational fluid dynamics
PC	Personal computer
C_u	Empirical constant
δ_{ij}	kronecker delta function
σ_ε& σ_k	Prandtl for turbulent kinetic energy
Re	Reynolds number $\left\{\frac{inertialresistance}{viscousresistance} = \frac{\rho v l}{\eta}\right\}$
Pr	Prandtl number$\left(\frac{\nu}{\propto} = \frac{Viscous\ diffusion\ rate}{thermal\ diffusion\ rate} = \frac{C_P \mu}{\kappa}\right)$
RANS	Reynolds Averaged Navier-Stokes Equations
ADI	Alternative Directional Implicit
FDE	Finite Difference Equation
Ar	Aspect Ratio

e	specific internal energy
L	Length of the enclosure
Ra	Rayleigh number
$\sigma_{k,1}$, $\sigma_{\omega,1}$, $\beta_{i,1}$	k-ω closure
$\sigma_{k,2}$, $\sigma_{\omega,2}$, $\beta_{i,2}$	k-ε closure
α_1 , β_{∞}^{*}	SST closure constants

Greek symbol

α	Thermal diffusivity, m^2/s
β	Thermal expansion coefficient, 1/k
ΔT	Temperature difference among cold and hot walls, k
v	Kinematic viscosity
μ	Dynamic viscosity
ξ	Non-dimensional temperature difference
ψ	Stream function
τ	Shear stress
ρ	Density of the fluid
Δt	Time interval
δ	Central difference operator
θ_f	Non-dimensional temperature difference $=\frac{T-T_c}{T_H-T_C}$
∂	Differential operator
∇	Del operator$i\frac{\partial}{\partial x}+j\frac{\partial}{\partial y}$

Subscript

b	Boundary value
c	Cold wall
h	Hot wall
i, j	$i^{th} and j^{th}$ Mesh points along the x and y direction respectively

Superscript

n	Current time step
$n+1$	New time step value
$-$	Mean value
$'$	Fluctuating component

ABSTRACT

Studies have been done on the aspect ratio effect on natural convection turbulence using standard k-ε model but further studies showed that *k-ω SST* model performed better than both *k-ε* and *k-ω* model in the whole enclosure. Thus, there was need to do a numerical study on the natural convection fluid flow in a rectangular enclosure full of air using *SST k-ω model*. The left vertical wall of the enclosure was maintained at a steady high temperature T_h of 323K while the right wall at a steady cool temperature T_c of 303K with the remaining walls adiabatic. Time-averaged energy, momentum and continuity equations with the two equation SST k-omega turbulence model were used to generate isotherms, streamlines and velocity magnitudes for different aspect ratios of the enclosure so as to be able to investigate effect of aspect ratio on turbulence. It was shown that as the aspect ratio of increased from 2, 4, 6 and 8 of the enclosure, the velocity of elements decreased and the vortices became smaller and more parallel thus concluded that an increase in aspect ratio decreased the turbulence.

CHAPTER ONE

1.1 INTRODUCTION

The mode of heat transfer in fluids (liquids and gases) is known as convection. When fluids are heated, they expand and thus density decreases. According to Archimedes' principle, warmer and lighter part of the fluid will lead to rise through the neighbouring cooler fluid.

According to Matthew P, Wilcox (2013), fluid stream can be categorized into two; turbulent and laminar flow. Motion of fluid elements in laminar flow is very organized and movement of fluid is in sheets that relatively slide on each other. The stream happens at very low speeds where there are just minor unsettling influences and low to no local speed variations.

Turbulence convection is an irregular or disturbed flow. It behaves with a chaotic and unpredictable motion. Turbulent convection in a fluid heated from a plane horizontal layer below, called Rayleigh-Bénard convection, is of great importance in several industrial and natural processes. The fluid becomes turbulent past a specific temperature difference.

Natural convection study in an enclosure has several engineering applications from natural space warming of household rooms to sections of engineering and atomic installations. Such as, this type of flows happens in material processing cooling of electronic equipment and building technology.

Turbulent flows are characterized by four main features: diffusion, dissipation, three-dimensionality and length scales. For numerical calculation of turbulent flows, an averaging of Navier-Stokes equations of motion is carried out with respect to time. This averaging leads to Reynolds Averaged Navier-Stokes equations (RANS). Additional terms with new variables occur in these partial differential equations because of the averaging. Consequently, there are suddenly more variables than equations. In order to close the motion equation system in this study, $k-\omega$ turbulence modeling will be used.

1.2 Problem statement

Turbulent flows are characterized by diffusion, dissipation, three-dimensionality and length scales. Studies on the effect of aspect ratio of a rectangular enclosure on natural convection turbulence using standard k-ε model has been done. However, SST k-ω model performs better than k-ω and k-ε since it combines both k-ω and standard k-ε models by activating the standard k-ω model near the wall and the k-ε model in the free stream thus ensuring right model is applied all through the

flow field. Since k-ε is normally suitable for free-shear layer flows and k-ω is used where there are wall effects present. This made a requirement to use a better turbulence model that would be useful both near the wall and in the free stream of the enclosure. Thus, a study on a rectangular enclosure, with one wall at 323K and the opposite one with 303k and the rest being remaining adiabatic, modeled using SST k-ω was done to investigate the turbulence in natural convection with the aspect ratio of 2, 4,6 and 8.

1.3 General objective

To investigate turbulent convection in a rectangular enclosure using SST k-ω model

1.4 Specific objectives

i) To develop numerical solutions for solving the model problems.
ii) To generate streamlines, isotherms and velocity magnitudes for different aspect ratio.
iii) To investigate the impact of aspect ratio on natural convection.

1.5 Significance of the Study

Many real-world applications uses natural convection in rectangular enclosures. Free cooling of air is the usual industrial use of natural convection and occurs on small scales such as computer chip all the way to large scale process tools. Where an enclosure is cooled and heated from one vertical edge to the other, at a small temperature difference, there is presence of the flow. The flow may be different near the walls and in the free stream thus a significant to use a model, SST k-ω, that will take care of both conditions. The behavior of Vortices as aspect ratio changes done in this study plays a significant in brine exclusion

1.6 Definition of terms

Convection: is heat transfer through movement of the heated sections of a fluid.

Aspect ratio: Proportion of length of isothermal wall to the gap between them

Heat transfer: The thermal energy exchange between temperature by distributing heat and physical systems relying upon the pressure.

Reynolds number: is the ratio of inertial forces to viscous forces within a fluid which is subjected to relative internal movement due to different fluid velocities.

Laminar Flow: A system where the fluid stream is smooth and regular for values of Reynolds number of up to about 2100

Turbulent Flow: A system of stream characterized by chaotic property changes flow for values of Reynolds number of above 4000

Streamlines: A path followed out by a massless component as it moves with the stream.

Isotherms: An isotherm is the curve on a graph that connects points of equal temperature.

Vortices: A region in the fluid medium where the flow is mostly rotating around an axis line.

Mathematical Formulation: translating the real-world problem into the form of mathematical equations which could be solved

Grashof number: a dimensionless number in fluid dynamics and heat transfer which approximates the ratio of the buoyancy to viscous force acting on a fluid

Prandtl number: a dimensionless parameter used in calculations of heat transfer between a moving fluid and a solid body,

Raleigh number: the product of the Grashof number and the Prandtl number.

FLUENT: is a "Flow Modeling Software" owned by and distributed by ANSYS, Inc. It is utilized to demonstrate fluid flow inside a characterized geometry utilizing the standards of computational fluid dynamics.

CHAPTER TWO

LITERATURE REVIEW

Numerical studies have been done on the development of natural convection in an enclosure. The choice region is common in numerous applications, for example, electronics (e.g. cupboards), applied chemistry (e.g. storing reservoirs) and ecological control (e.g. rooms).

Natural convection in rectangular enclosure cooled from the top limit while heated from one wall was studied by Aydin *et al*. (1999). They realized that the impact of Rayleigh number on heat transfer was more important when the enclosure is thin ($a_r > 1$) and the effect of aspect ratio is higher when the Rayleigh number is high and the enclosure is tall.

Betts & Bokhari (2000) found that stream fields and temperature to be closely two-dimensional, with the exception of anti-symmetric across the diagonal and near to the front and back walls of a tall differentially heated rectangular cavity. The partly conducting top and bottom give locally unsteady thermal stratification in the wall jet streams there, which develops the turbulence as the stream travels to the temperature-controlled plates.

Peng & Davidson (2001) studied turbulent natural convection stream ($Ra=1.58\times10^9$) in a restricted cavity with two differentially heated lateral boundaries. Large eddy simulation (LES) was used to investigate numerically. The mean stream in the cavity was described by steady thermal stratification and a moderately little turbulence level.

Bilgen (2002) used numerical technique to study turbulent and laminar natural convection in enclosures with fractional partitions. Horizontal boundaries were adiabatic while the vertical ones were isothermal. Two dimensional equations of conservation of energy, momentum and mass, with the Boussinesq approximation were solved.

A 3-D rectangular enclosure comprising of a convectional heater assembled into one wall and having an opening in the same wall study was done by Sigey *et al*. (2004). The heater was positioned under the opening and the rest of the walls were insulated. The heater location and dimensions were kept constant while the dimensions of the opening was varied and its location fixed. The localized heating and cooling initiates two limit sheets that collide in the area between the opening and the heater. They found that the enclosure was stratified into three sections: an

upper cold section, a warm lower section and a hot section in the area between the heater and the opening.

High Grashof-number turbulent natural convection in the region of vertical edges with heat transmission was analyzed asymptotically by Hölling & Herwig (2005). They found near-wall limit layer had a completely turbulent external layer and a viscosity-influenced internal layer, like the structure of forced convection limit layers.

Sharma *et al*. (2007) studied conjugate turbulent surface radiation and natural convection in rectangular enclosure cooled from other walls and heated from underneath, regularly experienced in Liquid Metal Fast Breeder Reactor (LMFBR) subsystems. The design contains the standard two equation k–ε turbulence model with physical limit conditions (no wall functions), along with the Boussinesq estimation, for the heat and stream transmission. As much as radiation is concerned, the radiosity – irradiation preparation for a transparent fluid of Prandtl number 0.7 was utilized. The conjugate coupling on the walls was taken care of by utilizing a fin type design. Based on the Rayleigh number was varied from 10^8 to 10^{12}, the aspect ratio ranging from 0.5 to 2.0 and the thickness of the enclosure.

The impacts of cavity aspect proportion, heat transmission qualities, depth of the exterior concrete beam, Rayleigh number (Ra) and exterior wall development materials on the stream were the key emphasis of the Ben-Nakhi & Mahmoud (2008) investigation. In their study of conjugate turbulent natural convection inside a building loft in the state of a rectangular enclosure limited by realistic walls, they found that the estimations of composite wall materials, Rayleigh number and loft aspect ratio have noteworthy impact on the stream function and temperature contours inside the enclosure, and the heat flux out of the room through the enclosure.

Xamán *et al*. (2008) used glass-walled square cavity. The cavity was such a way that one upright glass wall, one upright isothermal wall and two horizontal adiabatic walls. Using a control volume method to obtain the numerical outcomes in the cavity where the conditions were set as: 750 W/m^2 continuous direct normal solar irradiation over the glass wall, 35 °C outside ambient temperature and 21 °C even temperature in the isothermal wall. They found that the flow design was asymmetric because of joint impact of radioactive exchange within the cavity and non-isothermal glass wall.

Oztop & Abu-Nada (2008) studied heat transmission and fluid stream because of buoyancy forces in a partly heated enclosure using nanofluids utilizing different kinds of nanoparticles. Flush heater was placed to the left upright edge of limited length and the temperature of the heater to be higher than that of right upright wall while other walls were insulated. The governing equations were solved using the finite volume method. Heat transmission was as well increased with increase in height of heater. It was discovered that the heater position influences the stream and temperature fields when utilizing nanofluids and that the heat transmission was less noticeable at high aspect ratio than at low aspect ratio.

Braga, & de Lemos, (2009) did study on turbulent natural convection in a two-dimensional horizontal composite square cavity, cooled from the right side and isothermally heated at the opposite side and numerically analysed by use of finite volume technique. The composite square cavity was molded by three different regions, that is, solid, porous and clear region. They discovered that fluid starts to saturate the permeable medium for values of Ra more than 10^6. Nusselt number values demonstrated that for the range of Ra analysed, there is no noteworthy difference between laminar and turbulent models result. Comparison of impacts of Da, Ra and k_s/k_f on Nu showed that the solid phase properties have a more prominent impact in enhancing the general heat moved through the cavity.

Turbulent natural convection in a rectangular enclosure having limited width heat-conducting edges at local heating at the base of the cavity was numerically studied by Kuznetsov *et al***.** (2010). They carried out mathematical simulation in terms of the dimensionless RANS equations in stream function–vorticity designs. The design includes the standard two equation k–ε turbulence model with wall functions, alongside the Boussinesq estimation, for the heat and stream transmission.

Safaei *et al*. (2011) carried out numerical study on turbulent mixed and laminar convection in a shallow water-filled enclosure by different turbulence approaches. They initially demonstrated laminar mixed convection inside rectangular enclosure with moving edge and aspect ratio of 10 and after that the outcomes were related with other studies. The study was continued with turbulent flow using standard k-ε, RNG k-ε and RSM models for $Ra = 6 \times 10^9$ and Richardson numbers 0.1 to 10. The outcomes demonstrated that turbulence strength relies upon the location. For instance, stream in the center of enclosure was turbulent and in limit layer and upright walls, the

stream was laminar. Heat transfer and turbulence flow was generally more than laminar stream because of initial high level of mixing.

Chen & Du (2011) studied the impacts of aspect ratio, buoyancy forces ratio and thermal Rayleigh number on entropy generation of turbulent double-diffusive natural convection in a rectangle cavity. They concluded that the total entropy generation number (S_{total}) rises with Rayleigh number, S_{total} rises rapidly and linearly with buoyancy forces ratio and the relative total entropy generation rate because of diffusive irreversibility turn into dominant irreversibility and S_{total} rises almost linearly with aspect ratio.

Mahmoodi (2011) did heat and transmission mixed convection fluid stream in lid-driven rectangular enclosures filled with the Al_2O_3-water nanofluid. The right and left upright walls and upper horizontal wall of the enclosure were kept at a constant cold temperature Tc. The lower horizontal wall was kept at a constant hot temperature, with Th>Tc. The governing equations were solved by utilizing the finite volume technique and the SIMPLER algorithm. He found that at low Richardson values, an essential anticlockwise vortex was formed inside the enclosure and that for the range of the Richardson number considered, 10-1-101, increase in the volume fraction of the nanoparticles increased the average Nusselt number of the hot wall. It was too seen that the average Nusselt number of the hot wall of tall enclosures is higher to that of the shallow ones.

Sigey (2012) solved equations governing natural convection in a square enclosure. One wall was heated and cooled with the rest adiabatic. Discretization of governing equations together with the boundary conditions was utilized using second order central difference approximations in space and first order in time. The energy and vorticity transport equations were solved to the stable state utilizing Sarmaski-Andreyev (1963) Alternative-Direct Implicit (ADI). He found that turbulent limit layers formed on the cold and hot end wall.

Awuor (2013) studied performance of three numerical turbulence models in turbulent Convection Fluid Stream in an enclosure. The non-linear terms $\overline{u_i u_j}$ and $\overline{\theta i u}$ in the averaged energy and momentum equations respectively were modeled using the k–ε , k–ω and k–ω *SST* models to close the governing equations. He found that k –ω – *SST* model performed better than both k–ε and k–ω models in the whole enclosure. The k –ω – *SST* was then used in a test case problem of heating

and cooling on the same wall and found that the room was stratified into three sections: warm lower section, hot section in the area between the window and heater and a cold upper section.

Numerical study of natural convection surface and thermal radiation in a cubical cavity with a heat source situated at the base of the cavity with heat-conducting solid walls of fixed thickness was carried out by Martyushev & Sheremet (2014). Mathematical study in view of mathematical solution of the three-dimensional Boussinesq equations in the dimensionless parameters for instance temperature, vorticity vector and vector potential functions by finite difference technique was done and determined the effect scales of key parameters on the average Nusselt numbers.

Finite Volume Method was used to study the radiation impact on turbulent and laminar mixed convection heat transmission of almost transparent medium in a rectangular enclosure by Goodarzi *et al.* (2014). The simulated results showed that for laminar and turbulent motion states, computing the radiation heat transmission significantly improved the heat transfer coefficient as well as the Nusselt number (Nu). The average Nusselt number and corresponding heat transmission rate were not noticeably influenced by Higher Richardson numbers.

Wu. *et al*. (2015) investigated numerically the heat transmission and natural convective stream in a rectangular cavity full of heat-generating permeable medium. The right and left walls were partially cooled and heated by sinusoidal temperature profile and the bottom and top walls of enclosure were adiabatic. It was shown that periodic variations with negative and positive values show up in isotherms for solid and fluid phases, and periodicity rises with rise of *N*.

Wu *et al*. (2015) did a mathematical study of stable non-Darcy natural convection heat transmission in rectangular cavity full of heat-generating permeable medium with partial cooling by utilizing local thermal non-equilibrium (LTNE) model. The cooling parts of right and left sidewalls of the cavity were kept at temperature T_0 while the bottom and top walls of the enclosure, and also the inactive portions of its sidewalls, were kept insulated. The outcomes showed that the placement order of wall cooling significantly influence heat transmission rate and flow pattern. The comparison of fully cooled wall with partly cooled wall of the cavity produced a higher local Nusselt number for both solid and fluid phases.

Zdanski *et al*. (2016) studied the impacts of small rectangular turbulence promoter on convection heat transmission. The time-averaged energy, linear momentum and mass conservation governing

equations together with the two-equation k–ε turbulence model were utilized. The focus of the work was on the evaluation of the global and local Nusselt numbers at the channel stepped wall. They discovered that the highest local Nusselt number was situated in the section where the turbulent diffusion was highest in the near wall section.

A test investigation of stable buoyancy-driven convective heat transmission inside a slim triangular enclosure of aspect ratio 0.3175, between inclined cold wall and hot base plate while others wall being isothermal was investigated by Kumar *et al*. (2016). The Prandtl and Rayleigh numbers for various investigations were in the range 0.698 - 0.713 and $1779341 \leq Ra \leq 5559546$ respectively. It was revealed that Nusselt number is a great function of Rayleigh number and fin spacing while fin distance has moderate impact.

Hussen & Akeiber (2016) did mathematical analysis on radiative and convective heat transmission contrary to several partial floor heating in an enclosure. The temperature distribution in the heated places was found to be nearly similar to that of typical floor heating. But in the non-heated regions, air temperature varied by 6 °C (3.6 °C difference) between a point well above the floor and that close to the surface.

There has been a lot of research on heat convection turbulence in enclosures but not of heating from one wall and cooling from the opposite wall while taking into consideration of the near wall shear and in the free stream. Thus, a motivation towards our study towards the gap in numerical study on effect of aspect ratio on turbulent convection in rectangular enclosure using SST k-ω model which will take care of conditions of both the free stream and along the walls.

CHAPTER THREE

GOVERNING EQUATIONS

3.1 Continuity equation

Consider a control volume measuring $dx \times dy \times dz$

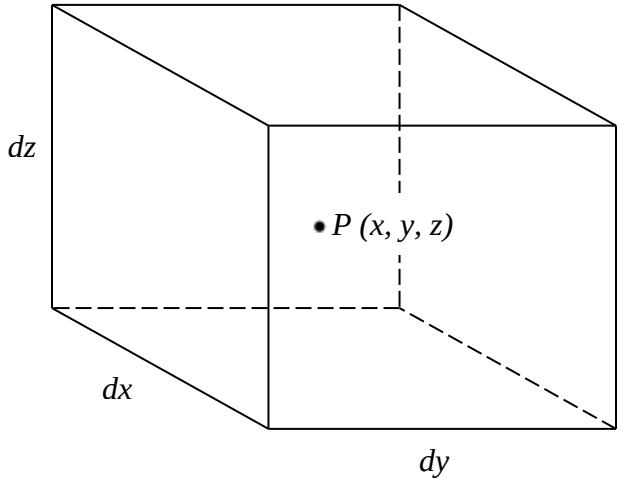

Fig. 3. 1 Control volume

Let the mass density at P(x, y, z) be ρ (x, y, z). Thus, average mass density throughout dv

Total mass = m = $\int \rho dv = \int \rho dx dy dz$ 3.1

Assuming inside dv there is no mass sinks or sources, then,

$\frac{dm}{dt}$= rate upon which mass leaves or enters through surface ds

The mass flux through the surface is ρV, where V represents velocity of the fluid. Thus, mass per unit time flowing through ds is

$\rho V \cdot ds = \rho V \cdot \hat{n} ds$ 3.2

where $\hat{n}$ is the unit vector orthogonal to the surface.

Total flow rate of mass out of the volume *dv* is

$\sum_{Faces} \rho V \cdot ds = \oint_s \rho V \cdot ds = \oint_s \rho V \cdot \hat{n} ds$ 3.3

And it's equivalent to$-\frac{dm}{dt}$, thus,

$\frac{dm}{dt} = \frac{d}{dt} \oint_v \rho dv = -\oint_s \rho \vec{V} \cdot \hat{n} ds$ 3.4

For fixed surface, derivative of total time within the volume integral can be taken as a partial derivative

$\int_v \frac{\partial \rho}{\partial t} dv = -\oint_s \rho \vec{V} \cdot \hat{n} ds$ 3.5

By Gauss theorem,

$$\oint_s \rho\vec{V} \cdot \hat{n}ds = \oint_v \nabla \cdot \left(\rho\vec{V}\right)dv \qquad 3.6$$

Thus substituting in equation (3.6) into (3.5), we get

$$\int_v \frac{\partial \rho}{\partial t} dv = -\int_v \nabla \cdot (\rho\vec{V})dv$$

$$= \int_v \left[\frac{\partial \rho}{\partial t} + \nabla \cdot (\rho\vec{V})\right] dv = 0 \qquad 3.7$$

Since it holds for any section and over any time interval, we conclude that the integrant in (3.7) must be identically be equal to zero, i.e.,

$$\frac{\partial \rho}{\partial t} + \nabla \cdot (\rho\vec{V}) = 0 \qquad 3.8$$

This is general equation of mass conservation.

For incompressible flows ρ is constant and equation 3.8 reduces to

$$\rho\nabla\vec{V} + \vec{V}\nabla\rho = 0$$

$$\rho\nabla\vec{V} = 0$$

$$\nabla\vec{V} = 0 \qquad \text{.....3.9}$$

For an incompressible flow, velocity field should be divergence free.

Since $\vec{V}$ is a velocity vector field, equation 3.9 can be written as;

$$\frac{\partial u}{\partial x} + \frac{\partial v}{\partial y} + \frac{\partial w}{\partial z} = 0$$

3.2 Momentum conservation equation

The equation results from Newton's second law of motion

$F = \mathrm{Ma}$

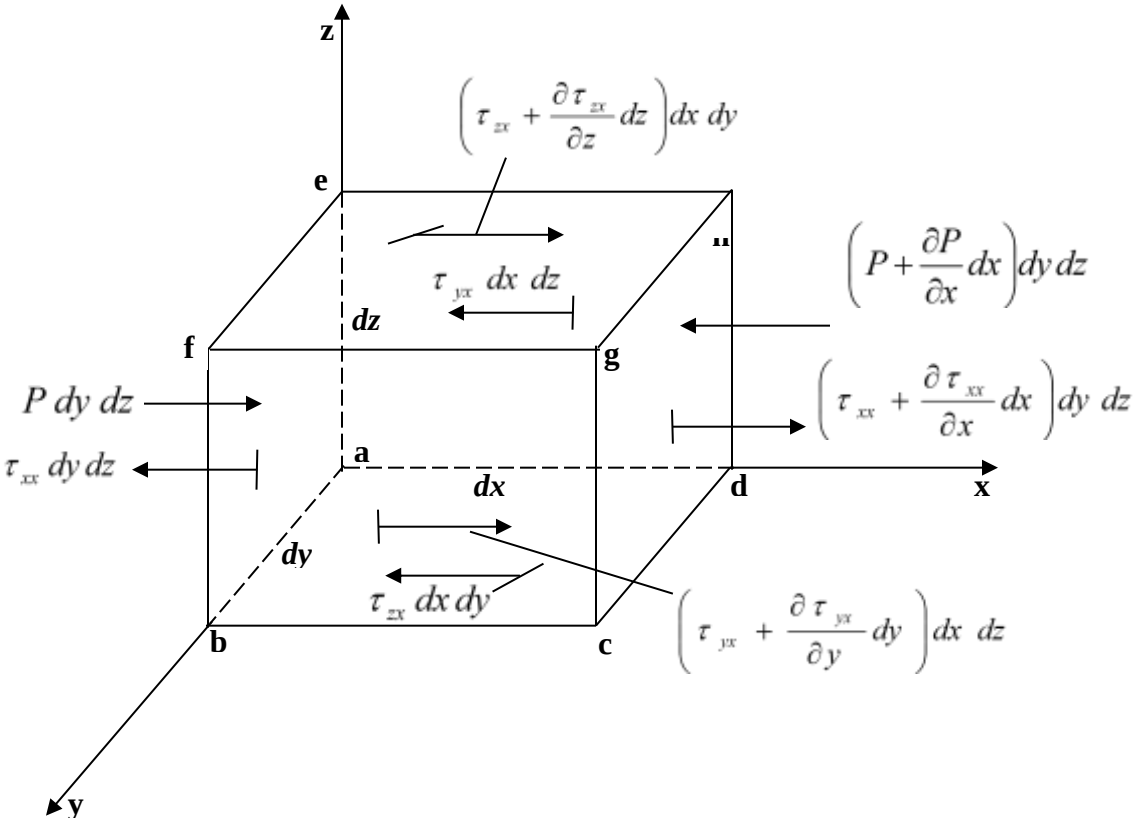

Fig. 3. 2 small moving fluid component showing forces in x course

The net force on fluid component equivalents to product of its acceleration and mass according to Newton's second law on the moving fluid component.

That is, $F = Ma$

Considering the x-component of the law,

$F_x = Ma_x$ 3.10

Where,

a_x - x-component of acceleration

F_x - x-component of force

Surface force (F_S) and body force (F_B) are the main forces acting on the component

Considering fluid component weight as the only body force and letting $\vec{g}$ the body force per unit mass acting on the fluid component, with g_x as the x-component, the weight of fluid component in the x-direction will be given by

$$F_B = \rho g_x(dxdydz) \qquad 3.11$$

Where $dxdydz$ is the volume of fluid component.

The surface force due to stress exerted on the sides of the fluid elements are the shear stress, normal stress and pressure.

The figure above shows the surface forces in x-course.

On face *abcd*, we have one shear force in negative x - course, $\tau_{zx}dxdy$and on the opposite face, the face *efgh* has a shear force of $\left(\tau_{zx} + \frac{\partial \tau_{zx}}{\partial z}dz\right)dxdy$in the positive x - course. Similarly for face *adhe*, we have $\tau_{yx}dxdz$acting in negative x - course and in the positive x - course we have $\left(\tau_{yx} + \frac{\partial \tau_{yx}}{\partial y}dy\right)dxdz$for the face *bcgf*.

For the face perpendicular to x-axis, that is, *abfe*, we have pressure force $Pdydz$ acting in positive x-direction and normal stress $\tau_{xx}dydz$ in negative x-direction while for the opposite face *cdhg* we have the pressure $\left(P + \frac{\partial P}{\partial x}dx\right)dydz$ acting against fluid element flow and normal shear $\left(\tau_{xx} + \frac{\partial \tau_{xx}}{\partial x}dx\right)dydz$ which acts in the positive x - course.

Thus, the sum of surface forces in x - course is

$$F_S = \left[\left(\tau_{xx} + \frac{\partial \tau_{xx}}{\partial x}dx\right) - \tau_{xx}\right]dydz + \left[P - \left(P + \frac{\partial P}{\partial x}dx\right)\right]dydz + \left[\left(\tau_{yx} + \frac{\partial \tau_{yx}}{\partial y}dy\right) - \tau_{yx}\right]dxdz + \left[\left(\tau_{zx} + \frac{\partial \tau_{zx}}{\partial z}dz\right) - \tau_{zx}\right]dxdy$$

$$F_S = \left(-\frac{\partial P}{\partial x} + \frac{\partial \tau_{xx}}{\partial x} + \frac{\partial \tau_{yx}}{\partial y} + \frac{\partial \tau_{zx}}{\partial z}\right)dxdydz \qquad 3.12$$

Thus, total forces in x - course F_x is obtained by summing equations 3.11 and 3.12

$$F_x = F_S + F_B$$

$$F_x = \left(-\frac{\partial P}{\partial x} + \frac{\partial \tau_{xx}}{\partial x} + \frac{\partial \tau_{yx}}{\partial y} + \frac{\partial \tau_{zx}}{\partial z}\right)dxdydz + \rho g_x dxdydz \qquad 3.13$$

Considering the R.H.S. of equation 3.10, the mass of the component is constant and is given by;

$$m = \rho dxdydz \qquad 3.14$$

The velocity components in the *z*, *y* and *x* directions of the fluid element is *w*, *v* and *u* respectively.

I.e. $w = \frac{dz}{dt}, \quad v = \frac{dy}{dt} \quad and \quad u = \frac{dx}{dt}$

the rate of change of velocity is the acceleration of the fluid component thus, a_x is the rate of change of u which is the acceleration component in the x-direction, thus,

$$a_x = \frac{du}{dt}$$

Thus,

$$F_x = \rho \frac{du}{dt} dxdydz \qquad 3.15$$

Combining eqns. 3.13 and 3.15 and dividing throughout by $dxdydz$, we get

$$\rho \frac{du}{dt} = -\frac{\partial P}{\partial x} + \frac{\partial \tau_{xx}}{\partial x} + \frac{\partial \tau_{yx}}{\partial y} + \frac{\partial \tau_{zx}}{\partial z} + \rho g_x \qquad 3.16a$$

Similarly, the y and z components becomes,

$$\rho \frac{dv}{dt} = -\frac{\partial P}{\partial y} + \frac{\partial \tau_{xy}}{\partial x} + \frac{\partial \tau_{yy}}{\partial y} + \frac{\partial \tau_{zy}}{\partial z} + \rho g_y \text{ and} \qquad 3.16b$$

$$\rho \frac{dw}{dt} = -\frac{\partial P}{\partial z} + \frac{\partial \tau_{xz}}{\partial x} + \frac{\partial \tau_{yz}}{\partial y} + \frac{\partial \tau_{zz}}{\partial z} + \rho g_z \qquad 3.16c$$

Equations 3.16a, b and c are x, y and z component of equation of momentum. The equations are in non-conservation form since the fluid component is moving with the flow, and thus in honour of Englishman G. Stokes and Frenchman M. Navier, they are called the Navier-Stokes equations.

Conservation form

The left side of eq.3.16a can be rewritten by introducing the vector notation

$$\nabla \equiv \vec{i}\frac{\partial}{\partial x} + \vec{j}\frac{\partial}{\partial y} + \vec{k}\frac{\partial}{\partial z}$$

Thus, the left hand side of equation 3.16a can be written as

$$\rho \frac{du}{dt} = \rho \frac{\partial u}{\partial t} + \rho \vec{V} \cdot \nabla u \qquad 3.17$$

Using the following derivative,

$$\frac{\partial(\rho u)}{\partial t} = \rho \frac{\partial u}{\partial t} + u \frac{\partial \rho}{\partial t}$$

$$\rho \frac{\partial u}{\partial t} = \frac{\partial(\rho u)}{\partial t} - u \frac{\partial \rho}{\partial t} \qquad 3.18$$

Using the divergence theorem,

$$\nabla \cdot \left(\rho u \vec{V}\right) = u \nabla \cdot \left(\rho \vec{V}\right) + \left(\rho \vec{V}\right) \cdot \nabla u$$

$$\rho \vec{V} \cdot \nabla u = \nabla \cdot \left(\rho u \vec{V}\right) - u \nabla \cdot \left(\rho \vec{V}\right) \qquad 3.19$$

Replacing eqns. 3.18 and 3.19 into eq. 3.17, we get

$$\rho \frac{du}{dt} = \frac{\partial(\rho u)}{\partial t} - u \frac{\partial \rho}{\partial t} - u \nabla \cdot \left(\rho \vec{V}\right) + \nabla \cdot \left(\rho u \vec{V}\right)$$

$$\rho\frac{du}{dt} = \frac{\partial(\rho u)}{\partial t} - u\left[\frac{\partial \rho}{\partial t} + \nabla\cdot\left(\rho\vec{V}\right)\right] + \nabla\cdot\left(\rho u\vec{V}\right)$$

3.20

Since the continuity equation is zero, hence the term in brackets in eqn. 3.20 is zero thus eqn. 3.20 simplifies to;

$$\rho\frac{du}{dt} = \frac{\partial(\rho u)}{\partial t} + \nabla\cdot\left(\rho u\vec{V}\right) \qquad 3.21$$

Replacing eqn. 3.21 into eqn. 3.16a, we get

$$\frac{\partial(\rho u)}{\partial t} + \nabla\cdot\left(\rho u\vec{V}\right) = -\frac{\partial P}{\partial x} + \frac{\partial \tau_{xx}}{\partial x} + \frac{\partial \tau_{yx}}{\partial y} + \frac{\partial \tau_{zx}}{\partial z} + \rho g_x$$

3.22a

Similarly, for Eqs. 3.16b and c we obtain,

$$\frac{\partial(\rho v)}{\partial t} + \nabla\cdot\left(\rho v\vec{V}\right) = -\frac{\partial P}{\partial y} + \frac{\partial \tau_{xy}}{\partial x} + \frac{\partial \tau_{yy}}{\partial y} + \frac{\partial \tau_{zy}}{\partial z} + \rho g_y$$

3.22b

and

$$\frac{\partial(\rho w)}{\partial t} + \nabla\cdot\left(\rho w\vec{V}\right) = -\frac{\partial P}{\partial z} + \frac{\partial \tau_{xz}}{\partial x} + \frac{\partial \tau_{yz}}{\partial y} + \frac{\partial \tau_{zz}}{\partial z} + \rho g_z \qquad 3.22c$$

The above equations are the conservation form of Navier-Stokes equations.

3.3 The Energy Equation

It results from first law of thermodynamics that states that the change in interior energy of a system is equivalent to the heat into the system less the work done by the system.

Mathematically it is expressed as

$$\Delta U = Q - W$$

Where W is the work done by the system, Q is the heat added to the system and ΔU is the change in internal energy.

i.e. $\begin{matrix}\textit{Rate of change}\\ \textit{of energy inside}\\ \textit{the fluid component}\end{matrix} = \begin{matrix}\textit{Net flux of}\\ \textit{heat into the}\\ \textit{component}\end{matrix} + \begin{matrix}\text{Rate of work done}\\ \textit{on the component due to}\\ \textit{surface and body forces}\end{matrix}$ …….. 3.23

We start by evaluating on moving fluid component, the rate of work done due to surface and body forces. It can be shown that the product of component of velocity in the direction of force and the force is equal to the rate of doing work by a force exerted on a body in motion.

Therefore, on the fluid component moving with speed **V,** the rate of work done by the body force is given by $\rho\vec{f}.\vec{v}$(dx dy dz)

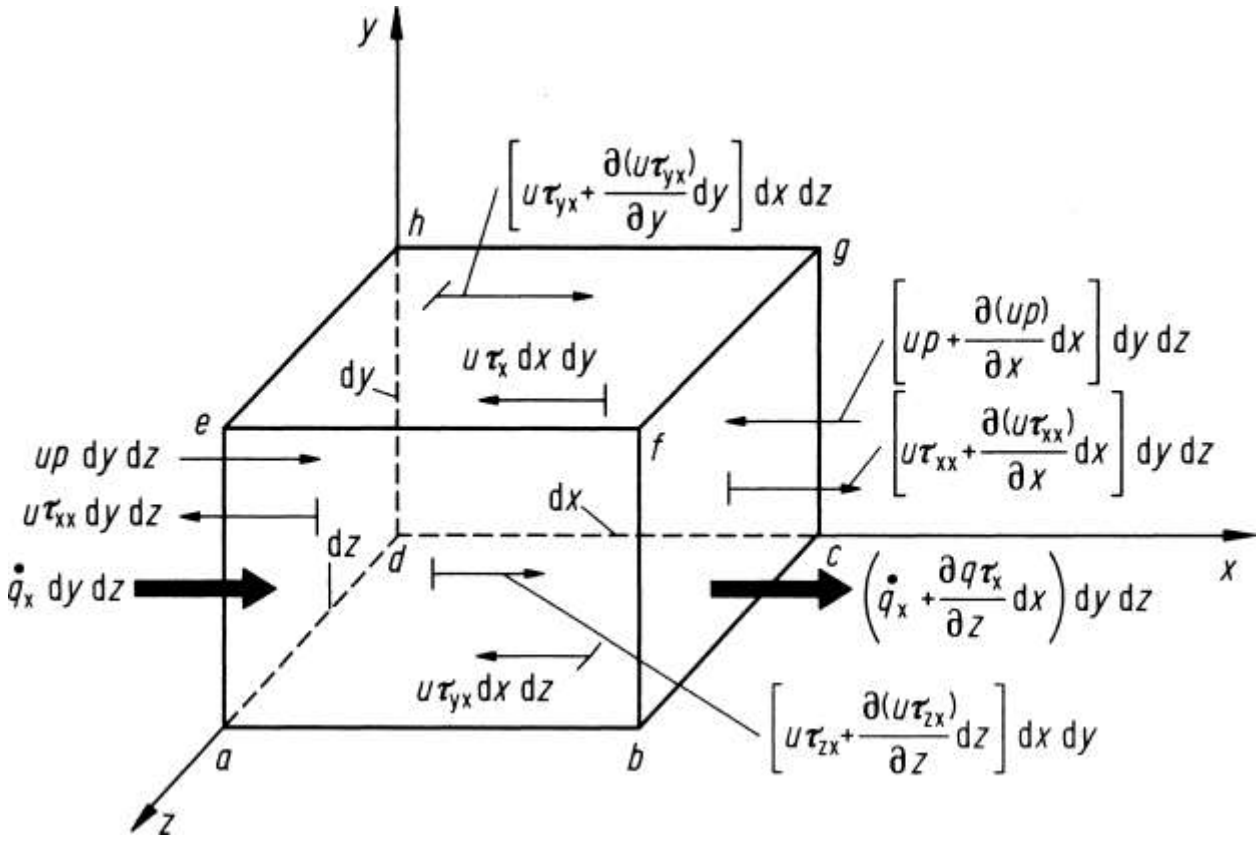

Fig. 3. 3 Energy transitions related with an imperceptibly little, moving fluid component.

We consider surface forces (pressure in addition to shear and normal stresses), acting in x-course (Figure 3.3). On the moving fluid component, the rate of work done by surface force in x - segment of speed u, duplicated by forces, for example, on *abcd* face, rate of doing work by τ_{yx}dxdz is uτ_{yx}dxdz with other faces having same expressions.

On fluid component, to acquire the total rate of doing work by surface force, it should be noted that negative work is done by forces in the negative x-course and positive work for positive x-course.

Considering the pressure force on the face 'bcgf' and 'adhe' in Figure 3.2, total rate of doing work by shear and pressure stress in x-course is given by

$\left[\text{up} - \left(up + \frac{\partial)(up)}{\partial x}\right)\right]$dydz= $-\frac{\partial(up)}{\partial x}$ dx dy dz,

and

$$\left[\left(u\tau_{yx}+\frac{\partial(u\tau_{yx})}{\partial y}\right)-u\tau_{yx}\right]dxdz=\frac{\partial(u\tau_{yx}}{\partial y}dxdydz$$

Bearing in mind all surface forces in figure 3.3, the net rate of doing work on the moving fluid component is;

$$\left[-\frac{\partial(up)}{\partial x}+\frac{\partial(u\tau_{xx})}{\partial x}+\frac{\partial\left(u\tau_{yx}\right)}{\partial x}+\frac{\partial(u\tau_{zx})}{\partial x}\right]dxdydz$$

This expression gives just surface forces in x- course; comparable expressions can be acquired for x- and z-courses. Incorporating the body force input and considering all surface forces, net rate of doing work on moving fluid component becomes,

$$\left\{\begin{matrix}Rate\ of\ workdone\\ on\ the\ element\ due\\ to\ the\ body\ forces\end{matrix}\right\}=\left[\begin{matrix}\left(\frac{\partial(up)}{\partial x}+\frac{\partial(vp)}{\partial y}+\frac{\partial(wp)}{\partial z}\right)+\\ \frac{\partial(u\tau_{xx})}{\partial x}+\frac{\partial(u\tau_{yx})}{\partial y}+\frac{\partial(u\tau_{zx})}{\partial z}+\\ \frac{\partial(v\tau_{xx})}{\partial x}+\frac{\partial(v\tau_{yy})}{\partial y}+\frac{\partial(v\tau_{zy})}{\partial z}+\\ \frac{\partial(w\tau_{xx})}{\partial x}+\frac{\partial(w\tau_{yy})}{\partial y}+\frac{\partial(w\tau_{zy})}{\partial z}\end{matrix}\right]\text{dxdydz}+\rho\vec{f}.\vec{v}\ldots\ldots\ldots\ldots\ldots\ldots\ldots 3.24$$

We now turn to the second term of equation (3.23), that is, net heat motion into the component. The volumetric warming causes heat transition, for example, ingestion or outflows of radiation, heat exchange over the surface because of temperature inclinations, that is, thermal conduction. We characterize q as the rate of accumulation of volumetric heat for each unit mass. As prior defined the mass of fluid component in motion in $\rho dxdydz,$ thus, we then acquire;

$$\left\{\begin{matrix}Volumetric\ heating\\ of\ the\ element\end{matrix}\right\}=\rho qdxdydz\ldots\ldots\ldots\ldots\ldots\ldots\ldots\ldots\ldots\ldots 3.25$$

In Figure 3.3, the heat exchanged into a moving fluid by thermal conduction component crosswise over face 'adhe' is $q_x$dxdydz where q_x is heat moved in x-course per unit area per unit time by thermal conduction. The heat exchanged out of the component crosswise over face 'bcgf' is,

$[\dot{q}_x+(\partial\, q_x/\partial x)dx]dydz,$

Therefore, the net moved heat by thermal conduction in the x-course into the fluid component is;

$$\left[\dot{q}_x - \left(\dot{q}_x + \frac{\partial q_x}{\partial x}\right) dx\right] dydz = -\frac{\partial \dot{q}_x}{\partial x} dxdydz$$

Considering heat exchanging the y-direction over other faces in fig 3.3, we acquire,

$$\left\{\begin{matrix}\text{Fluid component heating} \\ \text{by thermal conductivity}\end{matrix}\right\} = -\left(\frac{\partial \dot{q}_x}{\partial x} + \frac{\partial \dot{q}_y}{\partial y} + \frac{\partial \dot{q}_z}{\partial z}\right) \text{dx dy dz} \ldots\ldots\ldots\ldots\ldots\ldots\ldots\ldots\ldots\ldots\ldots\ldots 3.26$$

Summing up eqns (3.25) and (3.26), gives the net heat flux into the element;

$$\left\{\begin{matrix}\text{Fluid component heating} \\ \text{by thermal conductivity}\end{matrix}\right\} = \left[\rho\dot{q} - \left(\frac{\partial \dot{q}_x}{\partial x} + \frac{\partial \dot{q}_y}{\partial y} + \frac{\partial \dot{q}_z}{\partial z}\right)\right] \text{dx dy dz} \ldots\ldots\ldots\ldots\ldots\ldots\ldots\ldots\ldots 3.27$$

Local temperature corresponds to heat exchange by thermal conduction;

$$\dot{q}_x = -k\frac{\partial T}{\partial x}; \qquad \dot{q_y} = -k\frac{\partial T}{\partial y}; \qquad \dot{q}_z = -k\frac{\partial T}{\partial z};$$

Where k is the thermal conductivity.

Substituting these in equation (3.3.5) we have,

$$\left\{\begin{matrix}\text{Fluid component heating} \\ \text{by thermal conductivity}\end{matrix}\right\} = \left[\rho q - \frac{\partial}{\partial x}\left(k\frac{\partial T}{\partial x}\right) + \frac{\partial}{\partial y}\left(k\frac{\partial T}{\partial y}\right) + \frac{\partial}{\partial z}\left(k\frac{\partial T}{\partial z}\right)\right] \text{dx dy dz} \ldots\ldots\ldots\ldots 3.28$$

At last, we consider time rate of change of energy inside fluid component. Moving fluid aggregate energy for each unit mass is the entirety of its kinetic energy for each unit mass, $V^2/2$ and inner energy per unit mass, e. Thus, aggregate energy is $e + V^2/2$. Since the fluid component is in motion, the time-rate-of-change of energy for each unit mass is given by significant derivatives. Taking fluid component mass as $\rho dxdydz$, we have;

$$\left\{\begin{matrix}\text{Rate of change of} \\ \text{energy inside} \\ \text{the fluid element}\end{matrix}\right\} = \rho\frac{D}{Dt}\left(e + \frac{V^2}{2}\right) dxdydz \ldots\ldots\ldots\ldots\ldots\ldots\ldots\ldots\ldots\ldots\ldots\ldots\ldots\ldots\ldots\ldots\ldots\ldots 3.29$$

The last type of the energy is gotten by substituting eqns. (3.24), (3.28) and (3.29) into equation (3.23), obtaining;

$$\rho\frac{D}{Dt}\left(e+\frac{V^2}{2}\right)=\rho q+\frac{\partial}{\partial_x}\left(k\frac{\partial T}{\partial_x}\right)+\frac{\partial}{\partial_y}\left(k\frac{\partial T}{\partial_y}\right)+\frac{\partial}{\partial_z}\left(k\frac{\partial T}{\partial_z}\right)-\left(\frac{\partial[up]}{\partial_x}+\partial\frac{[vp]}{\partial_y}+\frac{\partial[wp]}{\partial_z}\right)+\frac{\partial[u\tau_{xx}]}{\partial_x}+\frac{\partial[u\tau_{yx}]}{\partial_y}+$$

$$\frac{\partial[u\tau_{zx}]}{\partial_y}+\frac{\partial[v\tau_{xy}]}{\partial_x}+\frac{\partial[v\tau_{yy}]}{\partial_y}+\frac{\partial[v\tau_{zy}]}{\partial_y}+\frac{\partial[w\tau_{xz}]}{\partial_x}+\frac{\partial[w\tau_{yz}]}{\partial_y}+\frac{\partial[w\tau_{zz}]}{\partial_y}+\rho\underset{f.}{\rightarrow}\underset{v}{\rightarrow}\text{……..…..….3.30}$$

This is the energy equation in non-conservation form. It's worth to note that it's in form of the total energy, $\left(e+\frac{v^2}{2}\right)$. Normally, the equation is written such that it involves the internal energy *e* which is derived as;

Rewriting equations 3.22 a, b and c as from Navier stoke, in non-conservative form, we have;

$$\rho\frac{Du}{Dt}=-\frac{\partial p}{\partial x}+\frac{\partial\tau_{xx}}{\partial x}+\frac{\partial\tau_{yx}}{\partial y}+\frac{\partial\tau_{zx}}{\partial z}+\rho f_x,$$

$$\rho\frac{Dv}{Dt}=-\frac{\partial p}{\partial y}+\frac{\partial\tau_{xy}}{\partial x}+\frac{\partial\tau_{yy}}{\partial y}+\frac{\partial\tau_{zy}}{\partial z}+\rho f_y, \qquad \text{……..3.31}$$

$$\rho\frac{Dw}{Dt}=-\frac{\partial p}{\partial z}+\frac{\partial\tau_{xz}}{\partial x}+\frac{\partial\tau_{yz}}{\partial y}+\frac{\partial\tau_{zz}}{\partial z}+\rho f_z.$$

Multiplying each of the equations, equation (3.31) by *u*, *v*, and *w* respectively,

$$\rho\frac{D\left(\frac{u^2}{2}\right)}{Dt}=-u\frac{\partial p}{\partial x}+u\frac{\partial\tau_{xx}}{\partial x}+u\frac{\partial\tau_{yx}}{\partial y}+u\frac{\partial\tau_{zx}}{\partial z}+\rho uf_x, \quad \text{……..3.32a}$$

$$\rho\frac{D\left(\frac{V^2}{2}\right)}{Dt}=-v\frac{\partial p}{\partial y}+v\frac{\partial\tau_{xy}}{\partial x}+\ v\frac{\partial\tau_{yy}}{\partial y}+v\frac{\partial\tau_{zy}}{\partial z}+\rho vf_y,\text{…….…….3.32b}$$

$$\rho\frac{D\left(\frac{V^2}{2}\right)}{Dt}=-w\frac{\partial p}{\partial y}+w\frac{\partial\tau_{xy}}{\partial x}+w\frac{\partial\tau_{yy}}{\partial y}+w\frac{\partial\tau_{zy}}{\partial z}+\rho vf_z,\text{…….……..…..3.32c}$$

Adding equations (3.32 a,b and c), and noting that $u^2+v^2+w^2=V^2$, we obtain;

$$\rho\frac{DV^2/2}{Dt}=-u\frac{\partial p}{\partial x}-v\frac{\partial p}{\partial y}-w\frac{\partial p}{\partial z}+u\left(\frac{\partial\tau_{xx}}{\partial x}+\frac{\partial\tau_{yx}}{\partial y}+\frac{\partial\tau_{zx}}{\partial z}\right)+v\left(\frac{\partial\tau_{xy}}{\partial x}+\frac{\partial\tau_{yy}}{\partial y}+\frac{\partial\tau_{zy}}{\partial z}\right)+w\left(\frac{\partial\tau_{xz}}{\partial x}+\right.$$

$$\left.\frac{\partial\tau_{yz}}{\partial y}+\frac{\partial\tau_{zz}}{\partial z}\right)+\rho(uf_x+vf_y+wf_z)\text{……..3.33}$$

Subtracting equation (3.33) from equation (3.30), noting that $\rho\overrightarrow{f}.\vec{v}=\rho(uf_x+vf_y+wf_z)$

We have;

$$\rho\frac{De}{Dt} = \rho q + \frac{\partial}{\partial x}\left(k\frac{\partial T}{\partial X}\right) + \frac{\partial}{\partial Y}\left(k\frac{\partial T}{\partial y}\right) + \frac{\partial}{\partial z}\left(k\frac{\partial T}{\partial z}\right) - p\left(\frac{\partial u}{\partial x} + \frac{\partial v}{\partial y} + \frac{\partial w}{\partial z}\right) + \tau_{xx}\frac{\partial u}{\partial x} + \tau_{yx}\frac{\partial u}{\partial y} +$$
$$\tau_{zx}\frac{\partial u}{\partial z} + \tau_{xy}\frac{\partial v}{\partial x} + \tau_{yy}\frac{\partial v}{\partial y} + \tau_{zy}\frac{\partial w}{\partial z} + \tau_{xz}\frac{\partial w}{\partial x} + \tau_{xz}\frac{\partial w}{\partial x} + \tau_{yz}\frac{\partial w}{\partial y} + \tau_{zz}\frac{\partial w}{\partial z} \quad \text{.....3.34}$$

In terms of internal energy, equation (3.34) is the energy equation. Note that it does not explicitly contain the body force when its written in terms of e, since the terms have cancelled. Still equation (3.34) is in non-conversation form. We note that

$\tau_{xy} = \tau_{yx} = \tau_{xz} = \tau_{zx} = \tau_{yz} = \tau_{zy}$, thus rewriting equation (3.34) we get,

$$\rho\frac{De}{Dt} = \rho q + \frac{\partial}{\partial x}\left(k\frac{\partial T}{\partial x}\right) + \frac{\partial}{\partial y}\left(k\frac{\partial T}{\partial y}\right) + \frac{\partial}{\partial z}\left(k\frac{\partial T}{\partial z}\right) - p\left(\frac{\partial u}{\partial x} + \frac{\partial v}{\partial y} + \frac{\partial w}{\partial z}\right) + \tau_{xx}\frac{\partial u}{\partial x} + \tau_{yy}\frac{\partial v}{\partial y} +$$
$$\tau_{zz}\frac{\partial w}{\partial z} + \tau_{yx}\left(\frac{\partial u}{\partial y} + \frac{\partial v}{\partial x}\right) + \tau_{zx}\left(\frac{\partial u}{\partial z} + \frac{\partial w}{\partial x}\right) + \tau_{zy}\left(\frac{\partial v}{\partial z} + \frac{\partial w}{\partial y}\right) \text{..... 3.35}$$

Using the definitions of normal the viscous stress and shear stress given (3.35) becomes,

$$\rho\frac{De}{Dt} = \rho q + \frac{\partial}{\partial x}\left(k\frac{\partial T}{\partial x}\right) + \frac{\partial}{\partial y}\left(k\frac{\partial T}{\partial y}\right) + \frac{\partial}{\partial z}\left(k\frac{\partial T}{\partial z}\right) - p\left(\frac{\partial u}{\partial x} + \frac{\partial v}{\partial y} + \frac{\partial w}{\partial z}\right) + \lambda\left(\frac{\partial u}{\partial x} + \frac{\partial v}{\partial y} + \frac{\partial w}{\partial z}\right)^2 +$$
$$\mu\left[2\left(\frac{\partial u}{\partial x}\right)^2 + 2\left(\frac{\partial v}{\partial y}\right)^2 + 2\left(\frac{\partial w}{\partial z}\right)^2 + \left(\frac{\partial u}{\partial y} + \frac{\partial v}{\partial x}\right)^2 + \left(\frac{\partial u}{\partial z} + \frac{\partial w}{\partial x}\right)^2 + \left(\frac{\partial v}{\partial z} + \frac{\partial w}{\partial y}\right)^2\right] \text{..... 3.36}$$

Equation (3.36) is a form of energy equation completely in terms of flow-field variables. Same replacement can be made into equation (3.30). In conservation form, the energy equation can be found as follows;

Considering the LHS of the equation (3.36) and from substantial derivative definition:

$$\rho\frac{De}{Dt} = \rho\frac{\partial e}{\partial t} + \rho V \cdot \nabla e, \text{.....3.37}$$

$$\frac{\partial(\rho e)}{\partial t} = \rho\frac{\partial e}{\partial t} + e\frac{\partial \rho}{\partial t} \text{Or } \rho\frac{\partial e}{\partial t} = \frac{\partial(\rho e)}{\partial t} - e\frac{\partial \rho}{\partial t} \text{.....3.38}$$

From the vector identity regarding divergence of the product of a vector and a scalar,

$$\nabla \cdot \left(\rho e\vec{V}\right) = e\nabla \cdot \left(\rho\vec{V}\right) + \rho\vec{V} \cdot e\nabla \text{.....3.39}$$

Substitute equations (3.38) and (3.39) into equation (3.37) we have;

$$\rho\frac{De}{Dt}=\frac{\partial(\rho e)}{\partial t}-e\left[\frac{\partial\rho}{\partial t}+\nabla\cdot\left(\rho\vec{V}\right)\right]+\nabla\cdot\left(\rho e\vec{V}\right)\text{……..3.40}$$

The expression in square brackets in equation (3.40) is zero

Thus, eqn (3.40) becomes

$$\rho\frac{De}{Dt}=\frac{\partial(\rho e)}{\partial t}+\nabla.\left(\rho e\vec{V}\right)\text{……..……..3.41}$$

Replacing eqn (3.41) into eqn (3.36), we get

$$\frac{\partial(\rho e)}{\partial t}+\nabla.\rho=\rho q+\frac{\partial}{\partial x}\left(k\frac{\partial T}{\partial x}\right)+\frac{\partial}{\partial y}\left(k\frac{\partial T}{\partial y}\right)+\frac{\partial}{\partial z}\left(k\frac{\partial T}{\partial z}\right)-p\left(\frac{\partial u}{\partial x}+\frac{\partial v}{\partial y}+\frac{\partial w}{\partial z}\right)+\lambda\left(\frac{\partial u}{\partial x}+\frac{\partial v}{\partial y}+\frac{\partial w}{\partial z}\right)^2+\mu\left[2\left(\frac{\partial u}{\partial x}\right)^2+2\left(\frac{\partial v}{\partial y}\right)^2+2\left(\frac{\partial w}{\partial z}\right)^2+\left(\frac{\partial u}{\partial y}+\frac{\partial v}{\partial x}\right)^2+\left(\frac{\partial u}{\partial z}+\frac{\partial w}{\partial x}\right)^2+\left(\frac{\partial v}{\partial z}+\frac{\partial w}{\partial y}\right)^2\right]\text{……..3.42}$$

Equation (3.42) is written in terms of the internal energy and is the energy equation in conservation form.

Similarly, in form of total energy, the conservation form of energy equation, can be written as;

$$\frac{\partial}{\partial t}\left[\rho\left(e+\frac{v^2}{2}\right)\right]+\nabla.\left[\rho\left(e+\frac{v^2}{2}\vec{v}\right)\right]=\rho q+\frac{\partial}{\partial x}\left(k\frac{\partial T}{\partial x}\right)+\frac{\partial}{\partial y}\left(k\frac{\partial T}{\partial y}\right)+\frac{\partial}{\partial z}\left(k\frac{\partial T}{\partial z}\right)-\frac{\partial(up)}{\partial x}-\frac{\partial(vp)}{\partial y}-\frac{\partial(wp)}{\partial z}+\frac{\partial(u\tau_{yx})}{\partial y}+\frac{\partial(u\tau_{zx})}{\partial z}+\frac{\partial(v\tau_{xy})}{\partial x}+\frac{\partial(v\tau_{yy})}{\partial y}+\frac{\partial(v\tau_{zy})}{\partial z}+\frac{\partial(w\tau_{xz})}{\partial x}+\frac{\partial(w\tau_{yz})}{\partial y}+\frac{\partial(w\tau_{zz})}{\partial z}+\rho\vec{f}.\vec{V}.$$

In Cartesian coordinate system, the governing equations for incompressible fluid flow become;

Mass conservation (continuity equation) equation

$$\frac{\partial u}{\partial x}+\frac{\partial v}{\partial y}+\frac{\partial w}{\partial z}=0$$

Momentum (Navier stokes) equations

X-direction:

$$\rho\left(\frac{\partial u}{\partial t}+u\frac{\partial u}{\partial x}+v\frac{\partial u}{\partial y}+w\frac{\partial u}{\partial z}\right)=F_X-\frac{\partial p}{\partial x}+\mu\left(\frac{\partial^2 u}{\partial x^2}+\frac{\partial^2 u}{\partial y^2}+\frac{\partial^2 u}{\partial z^2}\right)$$

Y-direction:

$$\rho\left(\frac{\partial v}{\partial t}+u\frac{\partial v}{\partial x}+v\frac{\partial v}{\partial y}+w\frac{\partial v}{\partial z}\right)=F_Y-\frac{\partial p}{\partial y}+\mu\left(\frac{\partial^2 v}{\partial x^2}+\frac{\partial^2 v}{\partial y^2}+\frac{\partial^2 v}{\partial z^2}\right)$$

Z-direction:

$$\rho\left(\frac{\partial w}{\partial t}+u\frac{\partial w}{\partial x}+v\frac{\partial w}{\partial y}+w\frac{\partial w}{\partial z}\right)=F_Z-\frac{\partial p}{\partial z}+\mu\left(\frac{\partial^2 w}{\partial x^2}+\frac{\partial^2 w}{\partial y^2}+\frac{\partial^2 w}{\partial z^2}\right)$$

Energy equation

$$\rho C_p\left(\frac{\partial T}{\partial t}+u\frac{\partial T}{\partial x}+v\frac{\partial T}{\partial y}+w\frac{\partial T}{\partial z}\right)=k\left(\frac{\partial^2 T}{\partial x^2}+\frac{\partial^2 T}{\partial y^2}+\frac{\partial^2 T}{\partial z^2}\right)+\mu\Phi\left\{2\left[\left(\frac{\partial \mathrm{u}}{\partial \mathrm{x}}\right)^2+\left(\frac{\partial \mathrm{v}}{\partial \mathrm{y}}\right)^2+\left(\frac{\partial \mathrm{w}}{\partial \mathrm{z}}\right)^2\right]+\left(\frac{\partial \mathrm{v}}{\partial \mathrm{x}}+\frac{\partial \mathrm{u}}{\partial \mathrm{y}}\right)^2+\left(\frac{\partial \mathrm{w}}{\partial \mathrm{y}}+\frac{\partial \mathrm{v}}{\partial \mathrm{z}}\right)^2+\left(\frac{\partial \mathrm{u}}{\partial \mathrm{z}}+\frac{\partial \mathrm{w}}{\partial \mathrm{x}}\right)^2\right\}$$

3.4 Reynolds Decomposition

The statistical averaging is necessary to estimate random fluctuations for time dependent nature of turbulence with extensive variety of scales.

This is a mathematical method that separates averaged and fluctuating part of the quantity, for instance, $u=\bar{u}+\grave{u}$ where $\bar{u}$ denotes time averaged of u known as steady part and $\grave{u}$ as the perturbations or fluctuating part. It lets us simplify the Navier Stokes Equations by replacing the sum of the fluctuating and steady part to the velocity profile and taking the average value. The equation that results comprises a non-linear called Reynolds stress which gives turbulence.

Statistical averaging of differential equations

The earliest attempts at developing Mathematical description the closure problem was performed by Boussinesq (1877) with introduction of concept of the eddy viscosity. The origin of time averaging NS equation dates back to the late 19th century when Reynolds (1895) published results from his research on turbulence.

The differential equations of energy, momentum and mass balances express fundamental physical laws and therefore hold for turbulent flow. If all the perturbations acting on the flow can be mathematically modeled, then these equations can be solved for the flow properties e.g. pressure

and velocity. An easier task is to solve time averaged versions of these equations in which some of the fluctuation contributions are averaged out.

$u = \bar{u} + \grave{u}$……...……3.4.1a

$v = \bar{v} + \grave{v}$……...……3.4.1b

$p = \bar{p} + \grave{p}$……...……3.4.1c

$\rho = \bar{\rho} + \grave{\rho}$……...……3.4.1d

$T = \bar{T} + \grave{T}$……...……...……3.4.1e

And time averaged rules

$\frac{1}{T}\int_0^T u dt = \bar{u}$ And $\frac{1}{T}\int_0^T \grave{u} dt = \bar{\grave{u}}$=0

$\frac{1}{T}\int_0^T v dt = \bar{v}$ And $\frac{1}{T}\int_0^T \grave{v} dt = \bar{\grave{v}}$=0

$\frac{1}{T}\int_0^T p dt = \bar{p}$ And $\frac{1}{T}\int_0^T \grave{p} dt = \bar{\grave{p}}$=0

$\frac{1}{T}\int_0^T \rho dt = \bar{\rho}$ And $\frac{1}{T}\int_0^T \grave{\rho} dt = \bar{\grave{\rho}}$=0

With T being a large interval of time.

The following rules as well apply during time averaging;

$\overline{\bar{f}}=\bar{f}$, $\overline{f+g} = \bar{f} + \bar{g}$, $\overline{\bar{f}.\bar{g}}=\bar{f}.\bar{g}$,

$\frac{\overline{\partial f}}{\partial s} = \frac{\partial \bar{f}}{\partial x}$, $\overline{\int f ds}=\int \bar{f}\, ds$, $\overline{f.g} \neq \bar{f}.\bar{g}$

Time averaged equation of continuity

Substituting 3.4.1b and 3.4.1d in 3.8 and time average, we obtain

$\overline{\frac{\partial(\bar{\rho}+\grave{\rho})}{\partial t} + \nabla.(\bar{\rho}+\grave{\rho})(\bar{v}+\grave{v})} = 0$……...……3.4.2

This gives

$\frac{\partial(\bar{\rho}+\overline{\rho})}{\partial t} + \nabla.\left(\overline{\bar{\rho}\bar{v}} + \overline{\bar{\rho}\grave{v}} + \overline{\grave{\rho}\bar{v}} + \overline{\grave{\rho}\grave{v}}\right) = 0$……...……3.4.3

But $\overline{\bar{\rho}\grave{v}}$, $\overline{\grave{\rho}}$ *and* $\overline{\grave{\rho}\bar{v}}$ *are equal to zero and* $\overline{\bar{\rho}\bar{v}} = \bar{\rho}\bar{v}$

So equation 3.4.3 becomes

$\nabla.\bar{v}$=0 (for incompressible fluid)……...……..…3.4.4

In Cartesian plane coordinate system, 3.4.4 becomes

$$\frac{\partial\overline{u}}{\partial x} + \frac{\partial\overline{v}}{\partial y} + \frac{\partial\overline{w}}{\partial z} = 0$$

Time averaged momentum equation

For a Newtonian, incompressible and with a constant viscosity fluid, Navier stokes equation 3.22 a and b we have;

$\rho\left(\frac{\partial v}{\partial t} + v.\nabla v\right) = F_i - \nabla p + \mu\Delta v$……...…….…….3.4.5

Substituting equations 3.4.1b and 3.4.1c in 3.4.5 and time averaging, we get

$$\overline{\rho\left[\frac{\partial(\bar{v}+\grave{v})}{\partial t} + (\bar{v}+\grave{v}).\nabla(\bar{v}+\grave{v})\right]} = F_i - \overline{\nabla(\bar{p}+\grave{p})} + \overline{\mu\Delta(\bar{v}+\grave{v})}$$

On working out, we get

$$\rho\left[\frac{\partial\overline{(\bar{v}+\grave{v})}}{\partial t} + \overline{\bar{v}.\nabla\bar{v}} + \overline{\bar{v}.\nabla\grave{v}} + \overline{\grave{v}\nabla\bar{v}} + \overline{\grave{v}.\nabla\grave{v}}\right] = F_i - \overline{\nabla\bar{p}} + \mu\Delta\bar{\bar{v}} + \mu\Delta\bar{\grave{v}}$$

Which gives

$\rho\left[\frac{\partial\bar{v}}{\partial t} + \bar{v}.\nabla\bar{v} + \overline{\grave{v}.\nabla\grave{v}}\right] = F_i - \overline{\nabla\bar{p}} + \mu\Delta\bar{v}$……...……3.4.6

Where$\overline{\bar{v}.\nabla\grave{v}}, \overline{\grave{v}\nabla\bar{v}}, \bar{\grave{v}}, \bar{\grave{p}}, \bar{\grave{v}}$ =0

And

$\nabla.\bar{v}$=0

$$\rho\left[\frac{\partial\bar{v}}{\partial t}+\bar{v}.\nabla\bar{v}+\overline{\nabla.\grave{v}\grave{v}}\right]=F_i-\overline{\nabla\bar{p}}+\mu\Delta\bar{v}$$

Which gives;

$$\rho\left[\frac{\partial\bar{v}}{\partial t}+\bar{v}.\nabla\bar{v}\right]=F_i-\overline{\nabla\bar{p}}+\mu\Delta\bar{v}-\overline{\nabla.\rho\grave{v}\grave{v}}\quad\text{……3.4.7}$$

$$\overline{\nabla.\rho\grave{v}\grave{v}}\ is\ called\ reynold\ stress\quad\text{……...……3.4.8}$$

In Cartesian plane coordinate system, the time averaged NS equations for all direction becomes;

X-direction:

$$\rho\left(\frac{\partial\bar{u}}{\partial t}+\bar{u}\frac{\partial\bar{u}}{\partial x}+\bar{v}\frac{\partial\bar{u}}{\partial y}+\bar{w}\frac{\partial\bar{u}}{\partial z}\right)=F_X-\frac{\partial\bar{\rho}}{\partial x}+\mu\left(\frac{\partial^2\bar{u}}{\partial x^2}+\frac{\partial^2\bar{u}}{\partial y^2}+\frac{\partial^2\bar{u}}{\partial z^2}\right)-\rho\left(\frac{\partial\overline{\grave{u}\grave{u}}}{\partial x}+\frac{\partial\overline{\grave{u}\grave{v}}}{\partial y}+\frac{\partial\overline{\grave{u}\grave{w}}}{\partial z}\right)$$

Y-direction;

$$\rho\left(\frac{\partial\bar{v}}{\partial t}+\bar{u}\frac{\partial\bar{v}}{\partial x}+\bar{v}\frac{\partial\bar{v}}{\partial y}+\bar{w}\frac{\partial\bar{v}}{\partial z}\right)=F_Y-\frac{\partial\bar{\rho}}{\partial y}+\mu\left(\frac{\partial^2\bar{v}}{\partial x^2}+\frac{\partial^2\bar{v}}{\partial y^2}+\frac{\partial^2\bar{v}}{\partial z^2}\right)-\rho\left(\frac{\partial\overline{\grave{u}\grave{v}}}{\partial x}+\frac{\partial\overline{\grave{v}\grave{v}}}{\partial y}+\frac{\partial\overline{\grave{v}\grave{w}}}{\partial z}\right)$$

Z-direction;

$$\rho\left(\frac{\partial\bar{w}}{\partial t}+\bar{u}\frac{\partial\bar{w}}{\partial x}+\bar{v}\frac{\partial\bar{w}}{\partial y}+\bar{w}\frac{\partial\bar{w}}{\partial z}\right)=F_Z-\frac{\partial\bar{\rho}}{\partial z}+\mu\left(\frac{\partial^2\bar{w}}{\partial x^2}+\frac{\partial^2\bar{w}}{\partial y^2}+\frac{\partial^2\bar{w}}{\partial z^2}\right)-\rho\left(\frac{\partial\overline{\grave{u}\grave{w}}}{\partial x}+\frac{\partial\overline{\grave{v}\grave{w}}}{\partial y}+\frac{\partial\overline{\grave{v}\grave{w}}}{\partial z}\right)$$

Time averaged energy equation

Substituting 3.4.1a, 3.4.1b, 3.4.1c &3.4.1e in

$$\rho C_p\left(\frac{\partial T}{\partial t}+u\frac{\partial T}{\partial x}+v\frac{\partial T}{\partial y}+w\frac{\partial T}{\partial z}\right)=k\left(\frac{\partial^2T}{\partial x^2}+\frac{\partial^2T}{\partial y^2}+\frac{\partial^2T}{\partial z^2}\right)+\Phi$$

We obtain

$$\rho C_p\left(\frac{\partial(\bar{T}+\grave{T})}{\partial t}+(\bar{u}+\grave{u})\frac{\partial(\bar{T}+\grave{T})}{\partial x}+(\bar{v}+\grave{v})\frac{\partial(\bar{T}+\grave{T})}{\partial y}+(\bar{w}+\grave{w})\frac{\partial(\bar{T}+\grave{T})}{\partial z}\right)=k\left(\frac{\partial^2(\bar{T}+\grave{T})}{\partial x^2}+\frac{\partial^2(\bar{T}+\grave{T})}{\partial y^2}+\frac{\partial^2(\bar{T}+\grave{T})}{\partial z^2}\right)+(\bar{\Phi}+\grave{\Phi})\quad\text{……...3.4.9}$$

Time averaging 3.4.9

$$\overline{\rho C_p\left(\frac{\partial(\bar{T}+\grave{T})}{\partial t}+(\bar{u}+\grave{u})\frac{\partial(\bar{T}+\grave{T})}{\partial x}+(\bar{v}+\grave{v})\frac{\partial(\bar{T}+\grave{T})}{\partial y}+(\bar{w}+\grave{w})\frac{\partial(\bar{T}+\grave{T})}{\partial z}\right)}=$$

$$\overline{k\left(\frac{\partial^2(\bar{T}+\grave{T})}{\partial x^2}+\frac{\partial^2(\bar{T}+\grave{T})}{\partial y^2}+\frac{\partial^2(\bar{T}+\grave{T})}{\partial z^2}\right)+(\bar{\Phi}+\grave{\Phi})}\ldots\ldots\ldots\ldots\ldots\ldots\ldots\ldots\ldots\ldots\ldots\ldots\ldots 3.4.10$$

These yields

$$\rho C_p\left(\frac{\partial\left(\overline{\bar{T}+\grave{T}}\right)}{\partial t}+\left(\overline{\bar{u}+\grave{u}}\right)\frac{\partial\left(\overline{\bar{T}+\grave{T}}\right)}{\partial x}+\left(\overline{\bar{v}+\grave{v}}\right)\frac{\partial\left(\overline{\bar{T}+\grave{T}}\right)}{\partial y}+\left(\overline{\bar{w}+\grave{w}}\right)\frac{\partial\left(\overline{\bar{T}+\grave{T}}\right)}{\partial z}\right)=k\left(\frac{\partial^2\left(\overline{\bar{T}+\grave{T}}\right)}{\partial x^2}+\frac{\partial^2\left(\overline{\bar{T}+\grave{T}}\right)}{\partial y^2}+\right.$$

$$\left.\frac{\partial^2\left(\overline{\bar{T}+\grave{T}}\right)}{\partial z^2}\right)+\left(\overline{\bar{\Phi}+\grave{\Phi}}\right)\ldots\ldots\ldots\ldots\ldots\ldots\ldots\ldots\ldots\ldots\ldots\ldots\ldots\ldots\ldots\ldots 3.4.11$$

Using the time averaged rules we get the following;

$$\rho C_p\left(\frac{\partial\bar{T}}{\partial t}+\bar{u}\frac{\partial\bar{T}}{\partial x}+\bar{v}\frac{\partial\bar{T}}{\partial y}+\bar{w}\frac{\partial\bar{T}}{\partial z}\right)=k\left(\frac{\partial^2\bar{T}}{\partial x^2}+\frac{\partial^2\bar{T}}{\partial y^2}+\frac{\partial^2\bar{T}}{\partial z^2}\right)-\frac{\partial c_p\overline{\grave{T}\grave{u}}}{\partial x_i}+\bar{\Phi}\ldots\ldots\ldots\ldots\ldots\ldots\ldots 3.4.12$$

$\frac{\partial c_p\overline{\grave{T}\grave{u}_i}}{\partial x_i}$ represent the turbulent heat fluxes i.e. perturbations of velocity and temperature

The stress tensor in turbulent flow

Equation 3.4.7 can be written in tensor form as

$$\rho\frac{D\overline{u_i}}{Dt}=F_i-\frac{\partial\bar{p}}{\partial x_i}+\mu\Delta\overline{u_i}-\rho\left(\frac{\partial\overline{u_iu_j}}{\partial x_i}\right)\ \ldots\ldots\ldots\ldots\ldots\ldots\ldots\ldots\ldots\ldots\ldots\ldots 3.4.13$$

Where $\mu\Delta\overline{u_i}-\rho\left(\frac{\partial\overline{u_iu_j}}{\partial x_i}\right)=\mu\frac{\partial}{\partial x_j}\left(\frac{\partial u_i}{\partial x_j}\right)-\rho\frac{\partial}{\partial x_j}\overline{u_iu_j}$

$$=\frac{\partial}{\partial x_j}\left(\mu\frac{\partial u_i}{\partial x_j}-\rho\overline{u_iu_j}\right)$$

The term in brackets in the above equation is known as total shear stress expressed as τ_{ij}.

Equation 3.4.7 can be written as

$$\rho \frac{D\overline{u_i}}{Dt} = F_i - \frac{\partial \bar{p}}{\partial x_i} + \frac{\partial}{\partial \mathrm{x_j}} \tau_{ij} \text{.........} 3.4.14$$

With the approach of *Eddy Viscosity principle*, equation3.4.14 is referred as Reynolds Averaged Navier Stokes equation (RANS).

And

$$\tau_{ij} = \mu \frac{\partial u_i}{\partial \mathrm{x_j}} + \rho \left(V_T \left(\frac{\partial u_i}{\partial x_j} + \frac{\partial u_j}{\partial x_i} \right) - {}^2\!/_3\, k\delta_{ij} \right) \text{.........} 3.4.15$$

Where δ_{ij} *is kronecker delta function*

V_T *is turbulent eddy viscosity*

3.5 Approach of Boussinesq

A relative old approach to this principle of eddy viscosity, which in 1877 was formulated by *Boussinesq* and is still the basis of many turbulence models (Rodi 1993).

$$-\overline{\grave{u}_i \grave{u}_j} = V_T \left(\frac{\partial u_i}{\partial x_j} + \frac{\partial u_j}{\partial x_i} \right) - {}^2\!/_3\, k\delta_{ij} \text{.........} 3.4.16$$

Where k is kinetic energy turbulence defined as

$$k = {}^1\!/_2 \left(\overline{u^2} + \overline{v^2} + \overline{w^2} \right) \text{.........} 3.4.17$$

Turbulent eddy viscosity, V_T, depends on the degree of turbulence i.e. it varies within the fluid flow and depending on the flow condition. The approach of calculating eddy viscosity V_T is known as turbulence modeling.

Applications and Approaches for turbulence modeling

The zeroth models, following the approach of Boussinesq (1877) assume that flow of velocity is proportional to turbulent stresses. In one equation model additional p.d.e for velocity scale is used for turbulence. Another p.d.e for length scale is added for two equation models. This group also includes K-ε and K-ω models. Approaches to determine the turbulence eddy viscosity provides the described closer models zeroth, first and second order.

3.6 Shear Stress Transport k-ω Model

It's a two-equation eddy – viscosity model. It combines the standard k-ω and k-ε models. It activates k-ε model in the free stream and standard k-ω model near the wall. This makes sure that the suitable model is applied all through the stream field.

The transport equations of SST k-ω model are;

$$\frac{\partial}{\partial t}(\rho k) + \frac{\partial}{\partial x_j}(\rho k u_i) = \frac{\partial}{\partial x_j}\left(\Gamma_k \frac{dk}{dx_j}\right) + \widetilde{G_k} - Y_k + S_k$$

And

$$\frac{\partial}{\partial t}(\rho \omega) + \frac{\partial}{\partial x_j}(\rho \omega u_i) = \frac{\partial}{\partial x_j}\left(\Gamma_\omega \frac{d\omega}{dx_j}\right) + G_\omega - Y_\omega + S_\omega + D_\omega$$

$\widetilde{G_k} = min(G_k, 10\rho\beta^* k\omega)$ - reproduction of turbulent kinetic energy owed to average velocity gradients where $G_k = -\rho\overline{u_i' u_j'}\frac{\partial u_j}{\partial x_i}$

$G_\omega = \frac{\alpha}{v_t} G_k$ is the generation of ω

D_ω denotes the cross-diffusion term.

Y_k and Y_ω denotes the dissipation of k and ω due to turbulence.

Γ_k and Γ_ω denotes the effective diffusivity of k and ω respectively.

For the SST k-ω model, the effective diffusivities are given by

$\Gamma_k = \mu + \frac{\mu_t}{\sigma_k}$ and $\Gamma_\omega = \mu + \frac{\mu_t}{\sigma_\omega}$

Where;

S_k and S_ω are user-defined source terms.

σ_ω & σ_k are turbulent Prandtl numbers for ω and k correspondingly.

Constants are determined from experiment and their values are as per the table 3.1 below.

Table 3. 1 Turbulence model constants

$\sigma_{k,1}$	1.176
$\sigma_{\omega,1}$	2.0
$\sigma_{k,2}$	1.0
$\sigma_{\omega,2}$	1.168
α_1	0.31
$\beta_{i,1}$	0.075
$\beta_{i,2}$	0.0828
$\boldsymbol{\alpha}_{\infty}^{*}$	1
α_{∞}	0.52
α_0	$\frac{1}{9}$
$\boldsymbol{\beta}_{\infty}^{*}$	0.09
R_{β}	8
R_k	6
R_{ω}	2.95
ζ^{*}	1.5
M_{to}	0.25

CHAPTER FOUR

4.1 Mathematical Formulation

Figure 4.1 demonstrates a graphic outline of the issue under thought and the coordinate structure. Considering a 2D rectangular structure of width W and height H, where the left vertical temperature is kept at T_h and the right at T_c, $T_h > T_c$. No heat stream is accepted at the upper and lower wall (adiabatic). The walls are unbending and no – slip circumstances are enforced at the limits.

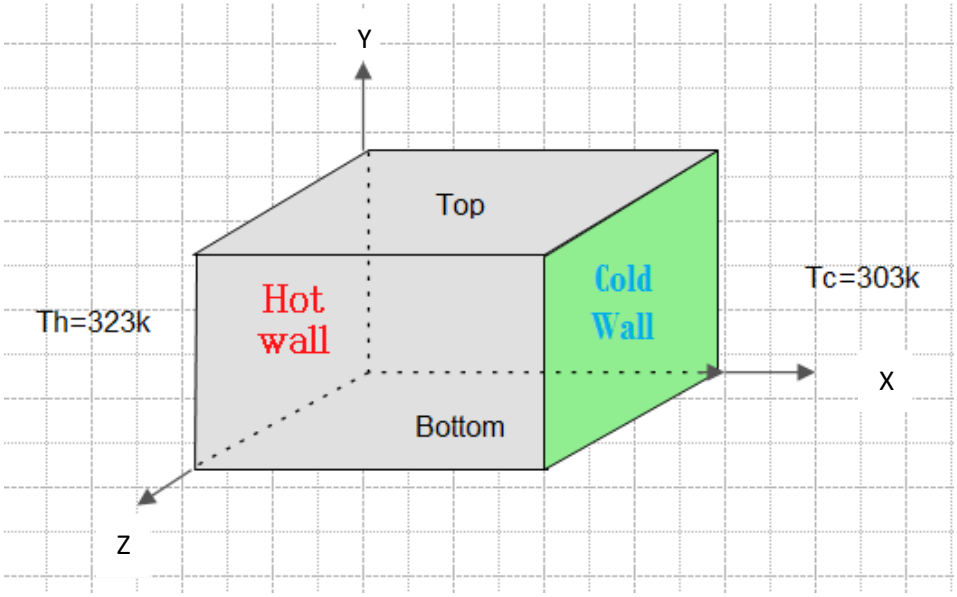

Fig. 4. 1 Geometry of the problem

4.2 Set of Governing equations

The representing equations in two dimensional rectangular directions;

$$\frac{\partial u}{\partial x} + \frac{\partial v}{\partial y} = 0 \quad \text{.....4.1}$$

$$\frac{\partial u}{\partial t} + u\frac{\partial u}{\partial x} + v\frac{\partial u}{\partial y} = F_x - \frac{\partial p}{\partial x} + \mu\left(\frac{\partial^2 u}{\partial x^2} + \frac{\partial^2 u}{\partial y^2}\right) \quad \text{.....4.2}$$

$$\frac{\partial v}{\partial t} + u\frac{\partial v}{\partial x} + v\frac{\partial v}{\partial y} = F_y - \frac{\partial p}{\partial y} + \mu\left(\frac{\partial^2 v}{\partial x^2} + \frac{\partial^2 v}{\partial y^2}\right) \quad \text{.....4.3}$$

$$\rho C_p\left(\frac{\partial T}{\partial t} + u\frac{\partial T}{\partial x} + v\frac{\partial T}{\partial y}\right) = k\left(\frac{\partial^2 T}{\partial x^2} + \frac{\partial^2 T}{\partial y^2}\right) + \Phi \quad \text{.....4.4}$$

Where

$$\Phi = \mu\left\{2\left[\left(\frac{\partial \mathrm{u}}{\partial \mathrm{x}}\right)^2 + \left(\frac{\partial \mathrm{v}}{\partial \mathrm{y}}\right)^2\right] + \left(\frac{\partial \mathrm{v}}{\partial \mathrm{x}} + \frac{\partial \mathrm{u}}{\partial \mathrm{y}}\right)^2\right\}$$

These conditions are legitimate for the present issue; despite that, density is a component of temperature. To change over the issue into an even state, Boussinesq estimation is usually utilized. Bousinesq estimation for limit layer streams and the current issue are depicted in the following two segments.

4.3. Limit Layer Streams Boussinesq Approximations

As constrained convection, the conditions that portray energy and momentum move in free convection starts from linked conservation ideologies. The distinction among the two streams is that, buoyancy forces play a noteworthy part in free convection. It is such powers that, truth be told, maintain the stream (Incropera and Dewitt 2002).

Adopting uneven, 2-D, consistent property circumstances where force of gravity act in the negative y course. Likewise, with one exemption, accept the liquid to be incompressible. The special case includes representing the impact of adjustable density in the force of buoyancy as it's this variety that initiates fluid movement. The last supposition is that the approximations of limit layer are legitimate. With the previous interpretations, for the uneven, 2-D stream of an incompressible fluid with consistent properties, y-momentum eqn 4.3 decreases to the limit layer eqn 4.5, apart from that the body constrain term f_y is held. On the off chance that the main commitment to this force is made by gravity, the body force for each unit volume is f_y = - g, with g as the neighborhood increasing speed because of gravity. Boussinesq estimation say that at every term of the equation of momentum, with the exception of the body constrain term, density is steady.

At that point, $\rho = \rho(T)$ for the body force.

$$\rho\frac{\partial v}{\partial t} + \rho u\frac{\partial v}{\partial x} + \rho v\frac{\partial v}{\partial y} = -\rho g - \frac{\partial p}{\partial y} + \mu\left(\frac{\partial^2 v}{\partial x^2} + \frac{\partial^2 v}{\partial y^2}\right) \quad \text{.....4.5}$$

Equation 4.5 might be framed in a more suitable method by first taking note of that from the x - momentum equation 4.2, $\frac{\partial p}{\partial x} = 0$ if there is no body force in x-course which implies no pressure change toward a path perpendicular to the surface. Henceforth the y-pressure slope anytime in the

limit layer must be equivalent to the pressure inclination. Be that as it may, in this locale $v = 0$ and the Eqn 4.5 diminishes to;

$$\frac{\partial p}{\partial y} = -\rho_\infty g \quad \text{.....4.6}$$

By substituting Eqn 4.6 into 4.5, resulting equation for momentum in y-course is acquired after executing some mathematical operations

$$\frac{\partial v}{\partial t} + u\frac{\partial v}{\partial x} + v\frac{\partial v}{\partial y} = g\left(\frac{\Delta\rho}{\rho}\right) + \mu\left(\frac{\partial^2 v}{\partial x^2} + \frac{\partial^2 v}{\partial y^2}\right) \quad \text{.....4.7}$$

Where $\Delta\rho = \rho_\infty - \rho$ and this applies at each section in the unrestricted convection limit layer. On the RHS of eqn. 4.7, buoyancy force is the first term and stream begin on the ground that density ρ is adjustable. In the event that variations of density are just owed to variations of temperature, the term might be associated to property of a fluid identified as coefficient of volumetric thermal expansion which is;

$$\beta \approx -\frac{1}{\rho}\left(\frac{\Delta\rho}{\Delta T}\right) \quad \text{.....4.8}$$

It gives a measure of the quantity by which the density change at steady pressure due to variation of temperature. It's stated in the estimated formula below;

$$\beta \approx -\frac{1}{\rho}\left(\frac{\Delta\rho}{\Delta T}\right) = -\frac{1}{\rho}\frac{\rho_\infty - \rho}{T_\infty - T} \quad \text{.....4.9}$$

It takes after that

$$\rho_\infty - \rho \approx \rho\beta(T_\infty - T) \quad \text{.....4.10}$$

This interpretation is identified as Boussinesq estimate and replacing it into Eqn 4.5, the y-momentum equation becomes;

$$\frac{\partial v}{\partial t} + u\frac{\partial v}{\partial x} + v\frac{\partial v}{\partial y} = g\beta(T_\infty - T) + \mu\left(\frac{\partial^2 v}{\partial x^2} + \frac{\partial^2 v}{\partial y^2}\right) \quad \text{.....4.11}$$

where it's presently clear how the bouyancy force, which drives the stream. The Boussinesq estimate is applied in natural convection in fluid dynamics which state that differences in density

are adequately little to be disregarded, aside from where they show up as multiples of g (gravitational acceleration).

4.4. Boussinesq Approximations for natural convection in a rectangular enclosure

For this work, there is not any of the body force in x-course and gravitational force g is the body force acting in negative y-course. If density varies just because of temperature differences (p=constant), Boussinesq estimation can be used into y-momentum eqn 4.5 by bearing in mind the dynamic and static pressures;

$$\rho\frac{\partial v}{\partial t}+\rho u\frac{\partial v}{\partial x}+\rho v\frac{\partial v}{\partial y}=-\frac{\partial p_{dynamic}}{\partial y}+\mu\left(\frac{\partial^2 v}{\partial x^2}+\frac{\partial^2 v}{\partial y^2}\right)-\frac{\partial p_{Static}}{\partial y}-\rho g\ldots\ldots\ldots\ldots\ldots\ldots\ldots\ldots..4.12$$

By introducing 4.10 into 4.12

$$\rho\frac{\partial v}{\partial t}+\rho u\frac{\partial v}{\partial x}+\rho v\frac{\partial v}{\partial y}=-\frac{\partial p_{dynamic}}{\partial y}+\mu\left(\frac{\partial^2 v}{\partial x^2}+\frac{\partial^2 v}{\partial y^2}\right)+\rho_\infty g-\rho g\ldots\ldots\ldots\ldots\ldots\ldots\ldots\ldots..4.13$$

Equation 4.13 can be rearranged to get $\rho_\infty-\rho$

$$\rho\frac{\partial v}{\partial t}+\rho u\frac{\partial v}{\partial x}+\rho v\frac{\partial v}{\partial y}=-\frac{\partial p_{dynamic}}{\partial y}+\mu\left(\frac{\partial^2 v}{\partial x^2}+\frac{\partial^2 v}{\partial y^2}\right)-g(\rho_\infty-\rho)\ldots\ldots\ldots\ldots\ldots\ldots\ldots4.14$$

And by using the relation 4.10 in 4.14, following can be obtained;

$$\rho\frac{\partial v}{\partial t}+\rho u\frac{\partial v}{\partial x}+\rho v\frac{\partial v}{\partial y}=-\frac{\partial p_{dynamic}}{\partial y}+\mu\left(\frac{\partial^2 v}{\partial x^2}+\frac{\partial^2 v}{\partial y^2}\right)+\rho g\beta(T_\infty-T)\ldots\ldots\ldots\ldots\ldots\ldots\ldots4.15$$

The Boussinesq assumptions made in this study (Boussinesq, 1903) include:

- All the fluid motion transport properties remain constant apart from density in the buoyancy term.
- The characteristic temperature ΔT be sufficiently small i.e. it tends to zero.
- The viscous dissipation effect is negligible
- The density varies linearly with temperature and the derivation from a reference value ρ_z is sufficiently small.

4.5. Dimensionless Energy, Momentum and Continuity Equations

Non – dimensionalizing governing equations makes equations simpler and highlights which terms are the most important. The main objective behind non–dimensionalization is to lessen number of

variables. The set of Equations 4.1, 4.2, 4.3 and 4.4 ought to be resolved to acquire the unknowns p, v, T and u. By applying Boussinesq estimation and then bringing up dimensionless constraints P, V, U, τ , θ, Y and X;

$X = \frac{x}{L}, Y = \frac{y}{L}, U = \frac{uL}{\alpha_f}, V = \frac{vL}{\alpha_f}, \theta_f = \frac{T_f - T_c}{T_h - T_c}., \tau = \frac{\alpha_f t}{L^2}$, p=$\frac{L^2 p}{\rho \alpha_f^2}$……..……4.16

The set of equation in dimensionless form becomes:

$\frac{\partial U}{\partial X} + \frac{\partial V}{\partial Y} = 0$……..…..……4.17

$\frac{\partial U}{\partial \tau} + U\frac{\partial U}{\partial X} + V\frac{\partial U}{\partial Y} = -\frac{\partial P}{\partial X} + Pr\left(\frac{\partial^2 U}{\partial X^2} + \frac{\partial^2 U}{\partial Y^2}\right)$……..……..4.18

$\frac{\partial V}{\partial \tau} + U\frac{\partial V}{\partial X} + V\frac{\partial V}{\partial Y} = -\frac{\partial P}{\partial Y} + Pr\left(\frac{\partial^2 V}{\partial X^2} + \frac{\partial^2 V}{\partial Y^2}\right) + Ra.Pr.\theta_f$……4.19

$\left(\frac{\partial \theta_f}{\partial \tau} + U\frac{\partial \theta_f}{\partial X} + V\frac{\partial \theta_f}{\partial Y}\right) = k\left(\frac{\partial^2 \theta_f}{\partial X^2} + \frac{\partial^2 \theta_f}{\partial Y^2}\right) + \Phi$……..……4.20

Where, Pr and Ra denotes Prantdl and Rayleigh numbers correspondingly; and θ_f the is dimensionless fluid temperature. In the next section, Grashof, Prandtl and Rayleigh number will be defined.

4.6. Meaning of Dimensionless Constraints

4.6.1. Prandtl Numbers

Is a proportion of the momentum diffusivity to thermal diffusivity ∝

$Pr = \frac{V}{\propto^2}$ ……..……4.21

It gives a degree of the comparative efficiency of energy and momentum transport by diffusion in the speed and thermal limit layers. When Prandtl value is near to 1, then the momentum and energy transmission by diffusion are equivalent. If it's less than 1, momentum diffusion rate is significantly exceeded by energy diffusion rate. The inverse is valid for Prandtl numbers more than 1. This shows that Prandtl value greatly effects the relative development of velocity and thermal limit sheets.

4.6.2. Grashof Number

Is the dimensionless number defined as;

$$Gr_l = \frac{g\beta(T_s - T_\infty)L^3}{V^2} \quad \text{.....4.22}$$

The Grashof number assumes a comparable part in free convection that Reynolds number play in constrained convection. The measure of proportion of inertia to viscid forces acting on a fluid components given by Reynolds number. Conversely, Grashof value shows the proportion of buoyancy forces to viscid force acting on the fluid.

4.6.3. Rayleigh Number

Noting that free convection limit layers aren't confined to laminar stream. Free convection streams ordinarily begin from a thermal unsteadiness i.e. hotter and less dense fluid rises upwards with respect to cooler and denser fluid. Nonetheless, for forced convection, hydrodynamic variabilities may likewise emerge. I.e., instabilities in the stream might be increased, prompting progress to turbulent from laminar stream. Change in free convection limit layers relies upon the relative size of viscid and buoyancy forces in the fluid. It is standard to correspond its event as far as the Rayleigh value, which is basically the result of Prandtl and Grashof number;

$$Ra_L = Gr_l Pr = \frac{g\beta(T_s - T_\infty)L^3}{v\propto} \quad \text{.....4.23}$$

The critical Rayleigh number for vertical plates is 10^8. Around this number shift to turbulence starts. According to Incropera and Dewitt (2002), turbulence strongly affects heat transmission that is why great importance is set on trial outcomes to get suitable correlations for turbulence stream where Rayleigh value is larger than 10^9.

4.7. Two Dimensional Flow vorticity defination

(Aksel 2003) defines vorticity vector,$\vec{\xi}$, as curl of speed vector,$\vec{V}$;

$$\vec{\xi} = curl\ \vec{V} = \nabla \times \vec{V} \quad \text{.....4.29}$$

For two-dimensional stream, Eqn 4.29 becomes;

$$\xi = \frac{\partial u}{\partial x} - \frac{\partial v}{\partial y} \quad \text{.....4.30}$$

All through the turning, the course of a fluid component changes however its location, shape and dimensions don't change. At the point when the liquid component moving in a stream field does not experience any pivot, at that point the stream is known to be irrotational. For irrotational stream;

$$\vec{\xi} = curl\,\vec{V} = \nabla \times \vec{V} = 0 \quad \text{.....4.31}$$

4.8. Streamfunction - Vorticity Relation and Vorticity Transport Equation

Differentiating dimensionless y-momentum eqn 4.19 w.r.t x and dimensionless x-momentum eqn 4.18 w.r.t y, eqn. 4.32 is arrived at after eliminating the dimensionless pressure term P by rearranging the derivatives;

$$\frac{\partial}{\partial \tau}\left(-\frac{\partial U}{\partial Y}+\frac{\partial V}{\partial X}\right)+U\frac{\partial}{\partial X}\left(-\frac{\partial U}{\partial Y}+\frac{\partial V}{\partial X}\right)+V\frac{\partial}{\partial Y}\left(-\frac{\partial U}{\partial Y}+\frac{\partial V}{\partial X}\right)=Pr\left[\left(\frac{\partial}{\partial X}\right)^2\left(-\frac{\partial U}{\partial Y}+\frac{\partial V}{\partial X}\right)+\left(\frac{\partial}{\partial Y}\right)^2\left(-\frac{\partial U}{\partial Y}+\frac{\partial V}{\partial X}\right)\right]+RaPr\frac{\partial \theta_f}{\partial X} \quad \text{.....4.32}$$

The dimensionless vorticity can be defined as;

$$\frac{\partial V}{\partial X}-\frac{\partial U}{\partial Y}=\Omega \quad \text{.....4.33}$$

After introducing the dimensionless vorticity4.33 into Equation 4.32;

$$\frac{\partial \Omega}{\partial \tau}+U\frac{\partial \Omega}{\partial X}+V\frac{\partial \Omega}{\partial Y}=Pr\left(\frac{\partial^2 \Omega}{\partial X^2}+\frac{\partial^2 \Omega}{\partial Y^2}\right)+RaPr\frac{\partial \theta_f}{\partial X} \quad \text{.....4.34}$$

Equation 4.34 is the vorticity transport condition. In the x and y momemntum, the pressure term is eliminated thus reducing the two equations to one. The dimensionless streamfunction can be defined as

$$U=\frac{\partial \psi}{\partial Y} \text{and } V=-\frac{\partial \psi}{\partial X} \quad \text{.....4.35}$$

$$\frac{\partial U}{\partial Y}=\frac{\partial^2 \psi}{\partial Y^2} \text{and } \frac{\partial V}{\partial Y}=-\frac{\partial^2 \psi}{\partial X^2} \quad \text{.....4.36}$$

From the definition of dimensionless vorticity 4.33 and by using 4.36;

$$\frac{\partial^2 \psi}{\partial X^2}+\frac{\partial^2 \psi}{\partial Y^2}=-\Omega \quad \text{.....4.37}$$

Equation 4.37 is the equation of streamfunction that's demonstrating the connection between dimensionless streamfunction and dimensionless vorticity.

4.9. Equation Sets in Streamfunction-Vorticity Form

By utilizing dimensionless streamfunction 4.35 and dimensionless vorticity 4.33 variables, eliminating pressure term in the equation of momentum, governing equations in dimensionless form are acquired. Using vorticity-streamfunction method, the resulting equations are used in finding unknown velocities and temperature values;

$$\frac{\partial \Omega}{\partial \tau} + \frac{\partial U\Omega}{\partial X} + \frac{\partial V\Omega}{\partial Y} = Pr\left(\frac{\partial^2 \Omega}{\partial X^2} + \frac{\partial^2 \Omega}{\partial Y^2}\right) + RaPr\frac{\partial \theta_f}{\partial X} \quad \text{4.38}$$

$$\frac{\partial^2 \psi}{\partial X^2} + \frac{\partial^2 \psi}{\partial Y^2} = -\Omega \quad \text{4.39}$$

$$\frac{\partial \theta_f}{\partial \tau} + \frac{\partial U\theta_f}{\partial X} + \frac{\partial V\theta_f}{\partial Y} = \frac{\partial^2 \theta_f}{\partial X^2} + \frac{\partial^2 \theta_f}{\partial Y^2} \quad \text{4.40}$$

In the equation 4.38, Rayleigh number is;

$$Ra = \frac{g\beta(T_h - T_c)L^3}{\nu\propto} \quad \text{4.41}$$

and the dimensionless vorticity and streamfunction are 4.33 and 4.35, respectively.

Although the boundary conditions become relatively complicated in such an indirect method to solution of Navier – Stokes equations, the vorticity – stream formulation is more attractive than the primitive variable formulation because:-

i. The number of differential equations to be solved is reduced.
ii. Continuity equation is automatically satisfied.
iii. It does not require staggered finite difference grid systems.

4.10 Boundary Conditions

The parameters of the approaching stream (dissipation of the turbulent kinetic energy ω, stream velocity or pressure and turbulent kinetic energy k) are viewed as known. The limit conditions suggested are:

$$\frac{U_\infty}{L} < \omega_{farfield} < 10\frac{U_\infty}{L}$$

$$\frac{10^{-5}U_\infty^2}{ReL} < k_{farfield} < \frac{0.1U_\infty^2}{ReL}$$

$$\omega_{wall} = 10\frac{6v}{\beta_1(\Delta d_1)^2}$$

$$k_{wall} = 0$$

Where L is the approximate length of computational area

In this study, temperature of the hot wall was kept at 323k and the other cold wall at 303k.

The operating temperature inside the enclosure of the air is 313k

The aspect ratio of the enclosure varied from 4m by 2m, 8 by 2m, 12m by 2m and 16m by 2m.

4.11 The k - ω Model of Turbulence

Is one of the frequently utilized turbulence models. This lets a 2 - equation model to justify for history impacts such as diffusion of turbulent energy and convection. For this work, the SST *k* – *ω* Model will be utilized. According to Menter (1993), the utilization of k-ω formulation in the internal sections of the limit layer makes the model straightforwardly usable all the way down to the wall through the viscid sub-layer, hence the SST k-ω model can be utilized as a low-re turbulence model with no additional damping function.

Thus, it was resolved that the SST *k* - *ω* model ought to be authenticated.

4.12 Buoyancy – driven and Natural Convection Flows

When a fluid heated and its density change with temperature a stream can be brought by gravitational force acting on the density differences. Such buoyancy – driven streams are called natural convection (or mixed – convection) streams and can be modeled by FLUENT.

4.13 Low – Reynolds Number Models

Turbulent unrestricted convection from a heated vertical wall is predicted using the standard forced stream modification by Gatheri (1994), Lin and Churchill (1978) require the insertion of a destruction term.

In the ε- equation it is necessary to include a generation term $2vv\left(\frac{\partial^2 u_j}{\partial x_k^2}\right)^2$

C_u and $C_{\varepsilon 2}$ are made function of R_t, turbulence Reynolds Number of $R_t = \frac{k^2}{v\varepsilon}$ which accounts for the Low – Reynolds impact on the stream region. The variation of C_u is determined by necessitating that the turbulence viscosity change as per Van Driest design in the near wall region. The variation of $C_{\varepsilon 2}$ is selected such that the model will correctly foresee the decay isotropic grid turbulence for both low and high turbulence intensities like in this case. Low – Reynolds number models are designed to maintain the high – Reynolds turbulence formulation in the Log – Law regions and fit measurement in the viscous sub – layer near walls. Parameters C_u and $C_{\varepsilon 2}$ are functions of Reynolds Number.

4.14 Boundary Conditions

4. 14.1 Temperature Boundary Conditions

The non – dimensional was defined by $\theta_f = \frac{T_f - T_c}{\Delta T_*}$ where ΔT_* is the characteristic temperature variance between hot and cold surfaces i.e. $\Delta T_* = T_h - T_c$, the choice of θ_f ensures that it is bounded and lie between 0 and 1. The thermal boundary conditions which were used are isothermal and adiabatic conditions. These conditions are represented by the equations:

$$\theta_f = constant$$

$$\frac{\partial \theta_f}{\partial n} = 0$$

Where n represents the direction perpendicular to a wall. Since the problem involves heating on one wall and cooling on the opposite wall all the remaining four walls of the enclosure are kept adiabatic on the cold and hot walls, the Derichlet boundary conditions are used where

$$\theta_{hot} = 1 \; and \; \theta_{cold} = 0$$

Neumann boundary condition is used on the remaining four walls i.e.$\frac{\partial \theta_f}{\partial n} = 0$ for each of four walls.

4. 14.2 Velocity Boundary Conditions

The conditions in the motion of fluid at a boundary are specified in terms of the velocity. Particles close to a surface do not move along with a flow when adhesive forces are stronger than cohesive forces. In a closed cavity each boundary is impermeable. Normal component of velocity at each boundary is zero. For example, the boundary x=0 in the Y-Z plane. The velocity component orthogonal to the surface is certainly zero as mass can't penetrate an impermeable solid surface.

The differential equations are solved by means of Fluent 6.3.26 program. The results obtained are presented and discussed in the next chapter. Recommendations on other areas that can be investigated are also given.

CHAPTER FIVE

NUMERICAL METHOD

5.1 Introduction

Fluid movement is guided by N–S equations, a set of nonlinear and coupled PDEs resulting from basic laws of conservation of energy, momentum and mass. The unknowns are generally temperature, pressure, stream velocity and density. The analytical solution of this equations is not possible henceforth in such situations, scientists resort to laboratory experiments. The results are generally qualitatively not the same as geometric and dynamical similitude are hard to apply at the same time between the laboratory experiment and prototype. Moreover, the plan and creation of these experimentations can be hard and expensive, especially for stratified spinning streams. CFD is a branch of fluid mechanics that uses data structures and numerical analysis to solve and analyze issues that involve fluid streams. Computers are utilized to play out the estimations necessary to simulate the interaction of fluids with surfaces defined by limit situations. Earlier, CFD was frequently contentious, as it included extra estimation to governing equations and brought up authentic problems. These days CFD is a well-known discipline along with experimental and theoretical approaches. This position is in substantial part because of the exponential development of PC control which has enabled us to handle ever bigger and more compound issues.

In CFD, the fundamental procedure is discretization. It's the way toward taking differential equations with unlimited amount of degrees of freedom and minimizing them to a limited degrees of freedom system. Subsequently, rather than solving all over and for all times, we will be contented with its calculation at definite time intervals and at limited number of locations. The partial differential equations are then reduced into algebraic equations system that can now be resolved. To guarantee that correct equations are being solved and that there is stability and convergence, there must be control of nature and characteristics of errors that may arise during the process of discretization process. Several discretization methods have been established to handle a variety of issues. They are spectral, finite volume, finite element and finite difference methods. We shall use finite difference methods for the purpose of this work.

5.2 Finite Difference Solution Method

It allows the dependent parameter values of a certain differential equation at all separate points in the computational area to be determined. The method employs the Taylor series expansion in

writing the derivative of a parameter as the difference among values of the parameter at several points in time or space.

Fig 5.1 shows a curve of u against x, i.e. $u(x)$. After discretization, the curve $u(x)$ can be represented by a set of separate points, u's where Taylor series expansion can be used to relate them to each other. Considering a small change Δx from point(i) for points $(i-1)$ and $(i+1)$.

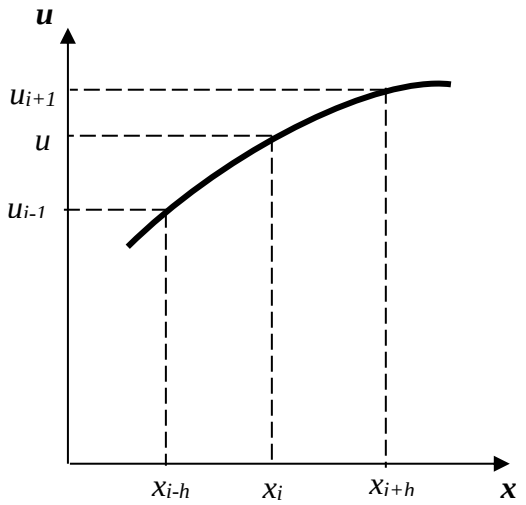

Fig. 5. 1 Location of points for Taylor series

Using Taylor series expansion about point (i), the velocity u_i can be expressed as:

$$u_{i+1} = u_i + \left[\frac{\partial u}{\partial x}\right]\Delta x + \frac{\partial^2 u}{\partial x^2}\frac{(\Delta x)^2}{2} + \left[\frac{\partial^3 u}{\partial x^3}\right]_i \frac{(\Delta x^3)}{6} + \ldots\ldots\ldots\ldots\ldots\ldots 5.1$$

And

$$u_{i-1} = u_i - \left[\frac{\partial u}{x}\right]\Delta x + \frac{\partial^2 u}{\partial x^2}\frac{(\Delta x)^2}{2} - \left[\frac{\partial^3 u}{\partial x^3}\right]_i \frac{(\Delta x^3)}{6} + \ldots\ldots\ldots\ldots\ldots\ldots\ldots\ldots\ldots\ldots\ldots\ldots 5.2$$

If Δx is little and number of terms are unlimited, then the above equations are numerically correct. Overlooking these terms prompts to a basis of error in the mathematical calculations as the equation for the derivatives is truncated and the error is known as truncation error. The truncation error for the second order accurate is expressed as:

$$\sum_{n=3}^{\infty}\left[\frac{\partial^n u}{\partial x^n}\right]_i \frac{(\Delta x)^{n-1}}{n!} \quad \ldots\ldots\ldots\ldots\ldots\ldots\ldots\ldots\ldots\ldots\ldots\ldots\ldots\ldots\ldots\ldots\ldots\ldots\ldots\ldots\ldots\ldots 5.3$$

By subtraction or addition of eqns. 5.1 and 5.2, the first and second derivatives at the central position i can be found. They are

$$[\frac{\partial u}{\partial x}]_i = \frac{u_{i+1}-u_{i-1}}{2\Delta x} - [\frac{\partial^3 u}{\partial x^3}]_i \frac{(\Delta x^3)^2}{6} \quad \text{..... 5.4}$$

And

$$[\frac{\partial^2 u}{\partial x^2}]_i = \frac{u_{i+1}-2u_i+u_{i-1}}{(\Delta x)^2} + o(\Delta x)^2 \quad \text{..... 5.5}$$

Equations 5.4 and 5.5 are known as central difference for first and second derivative, correspondingly. Bearing in mind eqns. (5.1) and (5.2) in isolation, more derivatives can also be formed. equation (5.1), the first order derivative can be formed as

$$[\frac{\partial u}{\partial x}]_i = \frac{u_{i+1}-u_i}{\Delta x} - [\frac{\partial^2 u}{\partial x^2}]_i \frac{(\Delta x)}{2} \text{..... .....5.6}$$

This is known as Forward difference. Likewise, from eqn (5.2) another-order derivative can be formed, i.e.

$$[\frac{\partial u}{\partial x}]_i = \frac{u_i-u_{i-1}}{\Delta x} - [\frac{\partial^2 u}{\partial x^2}]_i \frac{(\Delta x)}{2} \text{.....5.7}$$

This is referred as backward difference.

The distinguishing feature of a Finite Difference Method is estimation of the temporal $\frac{\partial \emptyset}{\partial t}$ and spatial $(\frac{\partial^2 \emptyset}{\partial x^2}, \frac{\partial^2 \emptyset}{\partial y^2})$ partial derivative in the governing equation with finite difference relating the values of the unidentified functions at a set of bordering grid points at several time-levels. Due to this approximation Partial Differential Equation (PDE) is replaced by the Finite-Difference Equation (FDE). The process of replacing the Partial Differential Equation with an algebraic Finite-Difference Equation is called Finite-Difference discretization or approximation.

Process of Finite-Difference discretization is done in two steps, namely discretization of the solution domain and discretization of governing equations.

5.3 Discretization of the Solution Domain

The stream in turbulent natural convection in an enclosure is characterised by a thin limit layer along the walls while the core is thermally stratified. A large quantity of grid points or computational nodes are required since the stream gradient is great in the limit layer, where the values of dependent parameters should be determined. In this study the primitive variable is used hence there is no need for a staggered finite difference grid system. The domain of the solution i.e., the enclosure is partitioned into a network of uniform rectangular grid with very fine spacing.

Figure 5.2 illustrates a 2-D computational area in Cartesian coordinate framework divided into small areas. The center to each subdivided area is a reference point called the node. There are four neighboring nodes for each node (i, j) in a 2-D computational area as shown in Fig. 5.3.

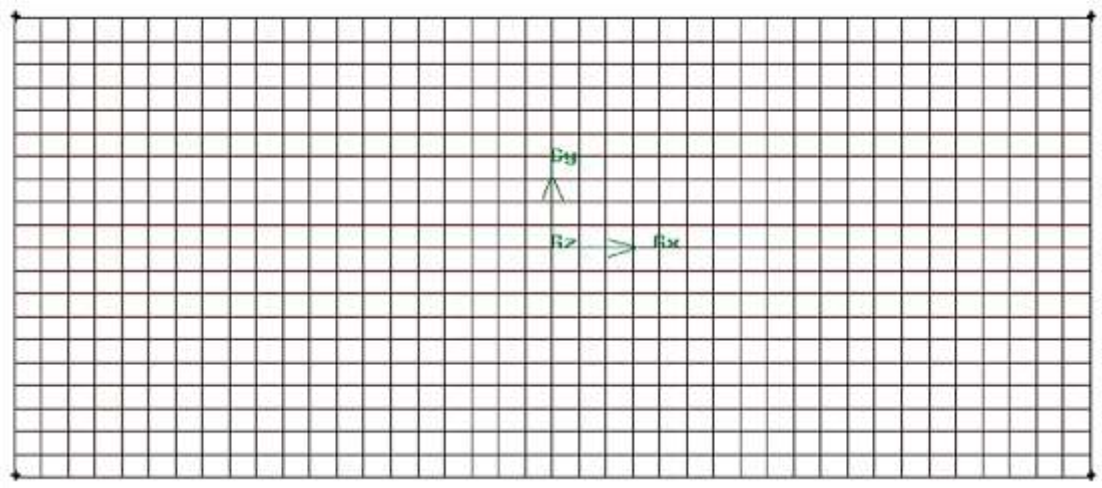

Fig. 5. 2 A two-dimensional Computational grid.

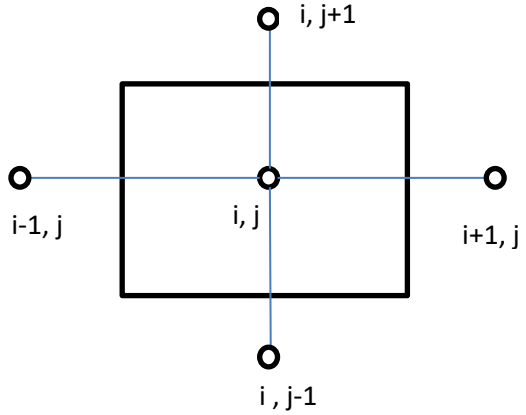

Fig. 5. 3 Cartesian coordinate showing a node (i,j) with its bordering nodes

5.4 Discretization of Governing Equations

This involves replacing governing equations with a finite-difference equation which is then applied sequentially at the internal nodes of the grid to give system of linear arithmetic equations that relate the estimation of unknown function $\emptyset$ at the nodes.

The goal of PDE with the FDE is to generate the estimations of the function $\emptyset$ at the nodes (i, j).

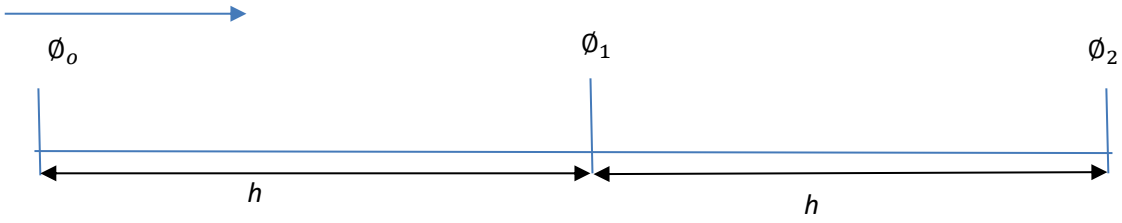

Fig. 5. 4 Three point Difference Approximation

$$\emptyset_2 = \emptyset_1 + h\emptyset' + \frac{h^2}{2}\emptyset'' + \frac{h^3}{6}\emptyset''' + o(h^4) \quad \text{.....5.8}$$

$$\emptyset_0 = \emptyset_1 - h\emptyset' + \frac{h^2}{2}\emptyset'' - \frac{h^3}{6}\emptyset''' + o(h^4) \quad \text{.....5.9}$$

Subtracting equation (5.9) from (5.8) yields

$$\emptyset_2 - \emptyset_0 = 2h\emptyset' + \frac{1}{3}h\emptyset''' + o(h^4) \quad \text{.....5.10}$$

Rearranging equation (5.10) we get

$$\emptyset' = \frac{\emptyset_2 - \emptyset_0}{2h} + o(h^4) \quad \text{.....5.11}$$

Adding equation (5.8) and (5.9) gives

$$\emptyset_2 + \emptyset_0 = 2\emptyset_1 + h^2\emptyset'' + o(h^4) \quad \text{.....5.12}$$

Rearranging the above equation results to

$$\emptyset'' = \frac{\emptyset_2 - 2\emptyset_1 - \emptyset_0}{h^2} + o(h^2) \quad \text{.....5.13}$$

Where h is the grid spacing.

Now, using Taylor series expansion in t to approximate the derivative of time $\frac{\partial \emptyset}{\partial t}$ with first order backward difference method about a node (i, j) at time instant t^{n+1} we get

$$\frac{\partial \emptyset}{\partial t} = \frac{\emptyset_{i,j}^{n+1} - \emptyset_{i,j}^{n}}{\Delta t} + o(\Delta t) \quad \text{.....5.14}$$

Using Taylor series expansion to approximate spatial derivatives with second order centered difference, we get

$$\frac{\partial^2 \emptyset}{\partial x^2} = \frac{\emptyset_{i-1,j}^{n+1} - 2\emptyset_{i,j}^{n+1} + \emptyset_{i+1,j}^{n+1}}{\Delta x^2} + o(h^2) \quad \text{.....5.15}$$

And

$$\frac{\partial^2 \emptyset}{\partial y^2} = \frac{\emptyset_{i,j-1}^{n+1} - 2\emptyset_{i,j}^{n+1} + \emptyset_{i+1,j}^{n+1}}{\Delta y^2} + o(h^2) \text{.....5.16}$$

The method above gives second order accuracy in spatial partial derivatives and first order accuracy in time.

Finite difference method allows spatial derivative of a differential equation for a grid point (i, j) to be written in terms of dependent variable values at that grid point and its neighboring grid points. Thus, the differential equation for point (i, j) can be diminished to an estimated arithmetic equation and the solution gives the dependent parameter value at point (i, j).

Likewise, discretization in time of the problem is necessary for us to attain the dependent parameter value of a differential equation that depends on time at any point in the computational area. Thus, time derivative of the differential equation ought to be in terms of values of dependent parameter and a time interval ought to be defined; for instance, toward the start and end moment of the time intervals. In this work, the superscript n denotes time dependence of dependent parameter.

5.6 Finite Difference Solution Technique for Parabolic Differential Equations

Since energy eqn 4.40 and the vorticity eqn 4.38 are alike, Mobedi (1994), they can be written in form of a single generic equation

$$\frac{\partial \emptyset}{\partial \tau} + U\frac{\partial \emptyset}{\partial X} + V\frac{\partial \emptyset}{\partial Y} = C\left(\frac{\partial^2 \emptyset}{\partial X^2} + \frac{\partial^2 \emptyset}{\partial Y^2}\right) + f \text{.....5.17}$$

Where $\emptyset$ is a generic dependent variable representing Ω.

Equation 5.17 can be reduced to the following form;

$$\frac{\partial \emptyset}{\partial \tau} = \delta_X^2 \emptyset + \delta_Y^2 \emptyset + f \quad \text{.....5.18}$$

In equation 5.18, $\delta_X^2 \emptyset \; and \; \delta_Y^2 \emptyset$ are

$$\delta_X^2 \emptyset = C \frac{\partial^2 \emptyset}{\partial X^2} - U \frac{\partial \emptyset}{\partial X} \quad \text{.....5.19}$$

$$\delta_Y^2 \emptyset = C \frac{\partial^2 \emptyset}{\partial Y^2} - V \frac{\partial \emptyset}{\partial Y} \quad \text{.....5.20}$$

Term $\delta_Y^2 \emptyset$ and $\delta_X^2 \emptyset$ denote convection and diffusion transport in Y and X direction correspondingly. Therefore, they can be referred as diffusion-convection terms. Several finite difference approaches can be used to solve the parabolic PDE. These approaches are commonly categorized into 3 categories, i.e., Alternating Direction Implicit (ADI), implicit and explicit approaches (Thiault 1985).

i) Explicit Methods:

When the method is applied on Eqn 5.18 for any point (i, j) in Cartesian coordinates when a simple forward difference for the time term is utilized can be expressed as;

$$\frac{\emptyset_{i.j}^{n+1} - \emptyset_{i,j}^{n}}{\Delta \tau} = \delta_X^2 \emptyset_{i,j}^{n} + \delta_Y^2 \emptyset_{i,j}^{n} + f_{i,j}^{n} \quad \text{.....5.21}$$

Where $\emptyset_{i,j}^{n}$ and $\emptyset_{i.j}^{n+1}$ denote the estimate of dependent parameter $\emptyset$ at node (i, j) at n^{th} and $(n+1)^{th}$ time steps, correspondingly. By taking the numerical spatial derivatives of dependent parameter in the preceding time step, n^{th} in Eqn 5.21 the unknown estimate of dependent parameter at point (i, j), $\emptyset_{i.j}^{n+1}$ can be found. Since values of the dependent parameter at all points of the computational area at n^{th} time step are identified, it's easy to determine the unknown $\emptyset_{i.j}^{n+1}$ in Eqn 5.21.

Propagation of the dependent parameter is done point by point in explicit method. According to Roach (1976), stability of the technique needs utilization of small-time interval or small grid dimensions which requires high PC storage and computational period.

ii) Implicit Method

Applying implicit technique wholly on eqn 5.18 for any point (i, j) in Cartesian coordinate, when a simple forward difference for time term is utilized, can be expressed as;

$$\frac{\emptyset_{i,j}^{n+1}-\emptyset_{i,j}^{n}}{\Delta\tau} = \delta_X^2\emptyset_{i,j}^{n+1} + \delta_Y^2\emptyset_{i,j}^{n+1} + f_{i,j}^{n+1} \quad \text{.....5.22}$$

In implicit technique, the spatial derivative of dependent parameter at the same time step determines the dependent parameter value at a new time step for a point (i, j), $\emptyset_{i,j}^{n+1}$. Therefore, m nodal equations must be acquired and solutions found so as the value of dependent parameter can be determined for a new time step in the computational area with m points. Thus, parabolic differential equation solution with implicit technique might be more complex compared to explicit technique.

Entirely implicit techniques are more required for computational fluid issues. According to Roach (1976), in entirely implicit techniques, in computational domain, propagation speed of dependent parameter is unlimited and thus becomes as genuinely stable techniques. solutions can be acquired for larger grid size or time interval compared to explicit techniques. Even though, implicit techniques are theoretically suitable for computational fluid issues, practically to get results solutions of large matrices must be performed.

iii) ADI method

The ADI method splits the finite difference equation into two, one having the x – direction and the other the y – direction. Every time step is divided into two sub-steps of equal duration $^1/_2\,\Delta t$ and approximating the spatial derivatives in a partially implicit manner while working sequentially and alternating in the x – and y – direction

For computational fluid problems, ADI techniques are more suitable than implicit techniques. As an alternative of large matrices, they offer simple tri-diagonal matrices of wholly implicit technique. According to Roach (1976), the tri-diagonal matrices can simply be solved by using Thomas Algorithm technique without any repetition. Mostly in an ADI method, for 2-D issues, parabolic differential equation, the Y course remains explicit while the equation is solved implicitly in X course. Similarly, the equation is solved implicitly in Y course. Thus, ADI technique decreases a 2-D implicit technique to a progression of 1-D implicit techniques.

Additionally, majority of ADI techniques are unconditionally steady techniques which allow the solution of parabolic differential equation for large time intervals and mesh sizes. The issue of this work is 2-D, to eliminate large matrices and to get higher order accuracy of the fully implicit technique. Use of ADI technique on Eqn 5.18 when simple forward difference for time term is utilized for any point (i, j) in Cartesian coordinate may be expressed in 2 stages as;

$$\frac{\emptyset_{i,j}^{n+1/2}-\emptyset_{i,j}^{n}}{\Delta\tau/2} = \delta_X^2\emptyset_{i,j}^{n+1/2} + \delta_Y^2\emptyset_{i,j}^{n} + f_{i,j}^{n} \quad \text{.....5.23}$$

$$\frac{\emptyset_{i,j}^{n+1}-\emptyset_{i,j}^{n+1/2}}{\Delta\tau/2} = \delta_X^2\emptyset_{i,j}^{n+1/2} + \delta_Y^2\emptyset_{i,j}^{n+1} + f_{i,j}^{n+1/2} \quad \text{.....5.24}$$

Where Eqn 5.23 is explicit for y - course and implicit for x - course and Eqn 5.24 is explicit for x - course and implicit for y - course. Solution of dependent parameter at a new time step $(n+1/2)^{th}$ for a point (i, j) , $\emptyset_{i,j}^{n+1}$ relies upon spatial derivatives of dependent parameter at the similar time step for x - course and the mathematical spatial derivative of dependent parameter in the preceding time step n^{th} for y - course. As a second step, the solution of dependent parameter at a new time step $(n+1)^{th}$ for point (i,j), $\emptyset_{i,j}^{n+1}$, relies on spatial derivatives of dependent parameter at similar time step for y - course and the mathematical spatial derivative of dependent parameter in the preceding time step $(n+1/2)^{th}$ for y - course.

Eqn 5.23 can be organized as;

$$\left(1-\frac{\Delta\tau}{2}\delta_X^2\right)\emptyset_{i,j}^{n+1/2} = \left(1+\frac{\Delta\tau}{2}\delta_Y^2\right)\emptyset_{i,j}^{n} + \frac{\Delta\tau}{2}f_{i,j}^{n} \quad \text{.....5.25}$$

Similarly, equation 5.24 can be arranged as

$$\left(1-\frac{\Delta\tau}{2}\delta_Y^2\right)\emptyset_{i,j}^{n+1} = \left(1+\frac{\Delta\tau}{2}\delta_X^2\right)\emptyset_{i,j}^{n} + \frac{\Delta\tau}{2}f_{i,j}^{n+1/2} \quad \text{.....5.26}$$

As it can be seen, the most important benefit of ADI technique is that result of the equations can be found after two stages with regard to a fully implicit technique.

5.7 Solver Execution

From the computer program Fluent 6.3.26. Menu is laid out such that order of operation is generally left to right and using the menu to get the solution we

- Imported and scaled mesh file
- Selected the physical models
- Defined material properties
- Prescribed operating conditions
- Prescribed boundary conditions
- Set solver controls
- Set up convergence monitors
- Computed and monitored the solution for convergence and accuracy

5.8 Solution Procedure Overview

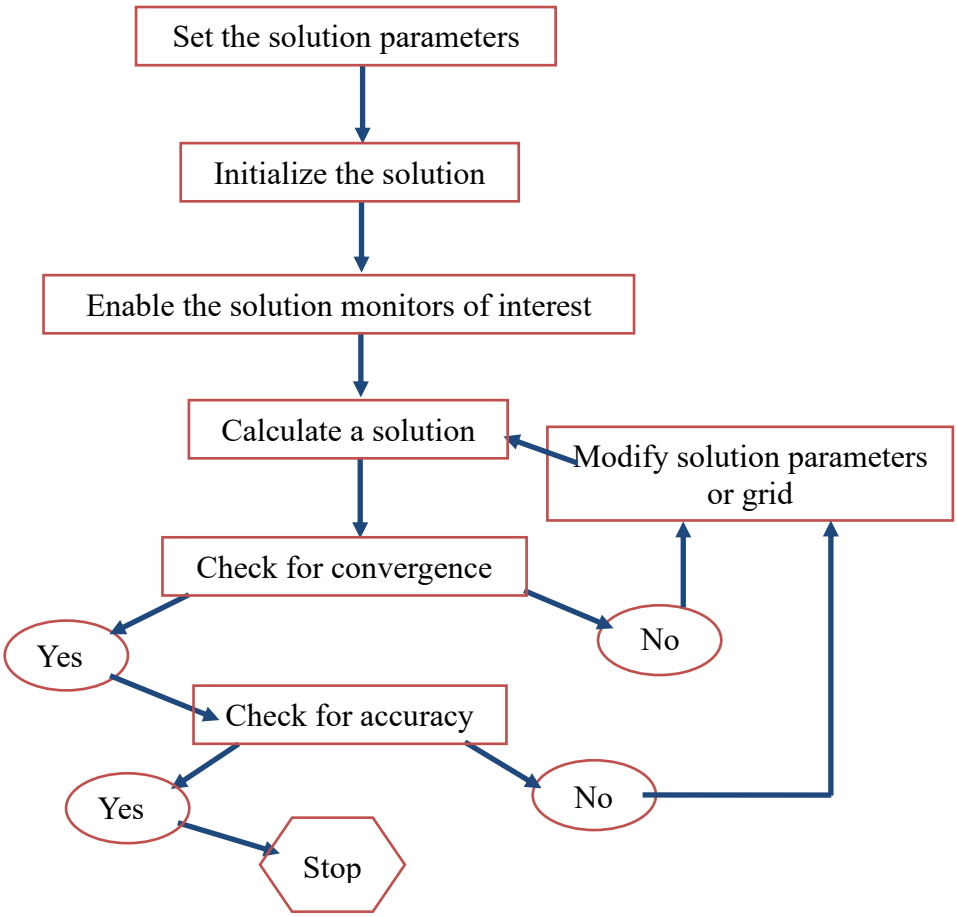

5.9 Turbulent flow important input

Table 5.1 shows the key input required to reproduce the outcomes shown in chapter six.

Table 5. 1 Turbulent flow variable inputs

Input	Value
Geometry	
Aspect ratio 2	4 by 2
Aspect ratio 4	8 by 2
Aspect ratio 6	12by 2
Aspect ratio8	16 by 2
Models	
Energy	on
Viscous	SST k-ω
Material Properties (Air)	
Density	1.1275 kg/m^3
Dynamic Viscosity	19148E-5 kg/m-s
Specific Heat Capacity	1.0069E+3J/Kg/K
Thermal conductivity	0.027076W/m/k
Thermal expansion coefficient	3.1934E-3
Solution Methods	
Pressure	PRESTO
Momentum	First Order Upwind
Turbulent Kinetic Energy	First Order Upwind
Turbulent Dissipation Rate	First Order Upwind

CHAPTER SIX

Results and Discussions

The results presented here were obtained by resolving the governing equations mathematically by utilizing Finite Difference Technique and together with the boundary situations give the numerical solutions for variables in SST $\kappa - \omega$ model.

In this study, height is kept constant at 2m while changing the distance between two isothermal walls i.e. the right and left walls which in this case is referred as the aspect ratio. It is varied at a sequence of even numbers (2, 4, 6 and 8) and results of isotherms, stream lines and contours of velocity magnitudes are recorded at z = 0.5.

6.1 Isotherms

Isotherm is a line of equal or constant temperature or is a curve on a graph that connects points of equal temperature.

In figure 6.1.1, the maximum temperature is 117K, in 6.1.2, the highest temperature is 56.7K, 6.1.3, the highest temperature is 42.6K and in 6.1.4, the highest temperature is 34.2K. The high temperatures are evident on the left side wall. In all cases two round motion in opposite directions (anticlockwise and clockwise direction). There is rises up of hot less dense particles which losses its heat with distance as shown by change in color. In between the two isothermal walls there is mixing of air particles which is a region of thermal equilibrium and is a relatively warm region. In 16 c and d, temperature uniformity is achieved. In conclusion, it is evident that maximum temperature decreases with increase in aspect ratio.

Fig. 6.1. 1 Isotherm of aspect ratio 2

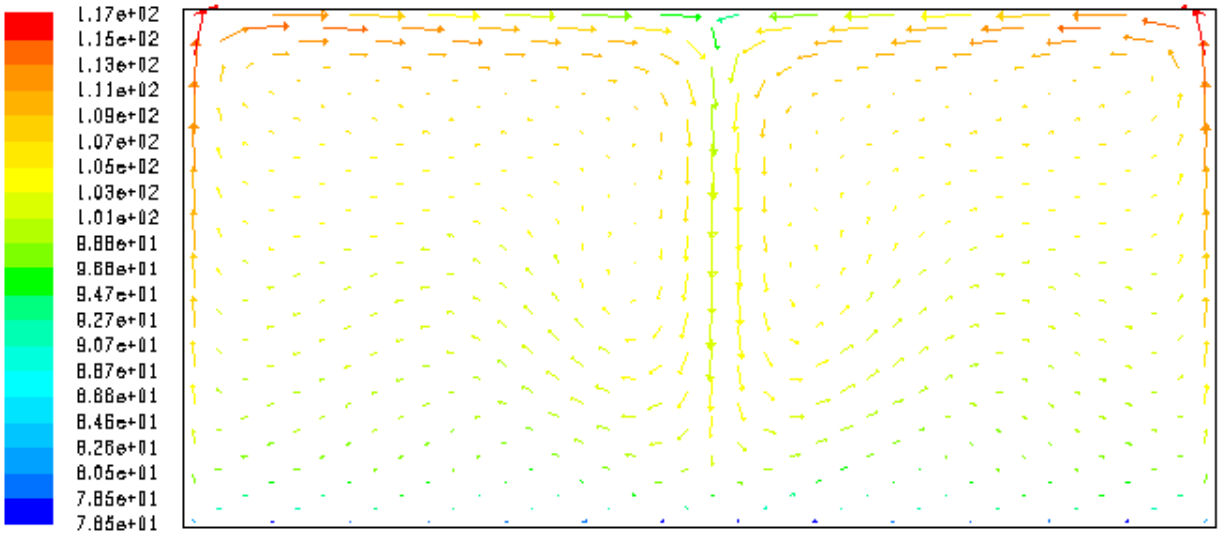

Fig. 6.1. 2 Isotherm of aspect ratio 4

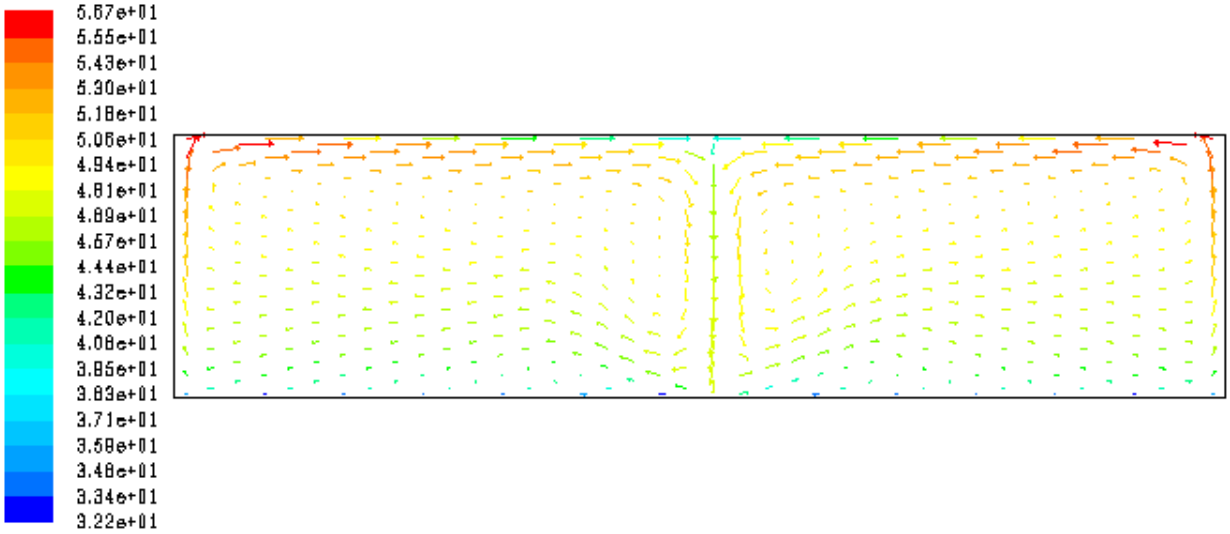

Fig. 6.1. 3 Isotherm of aspect ratio 6

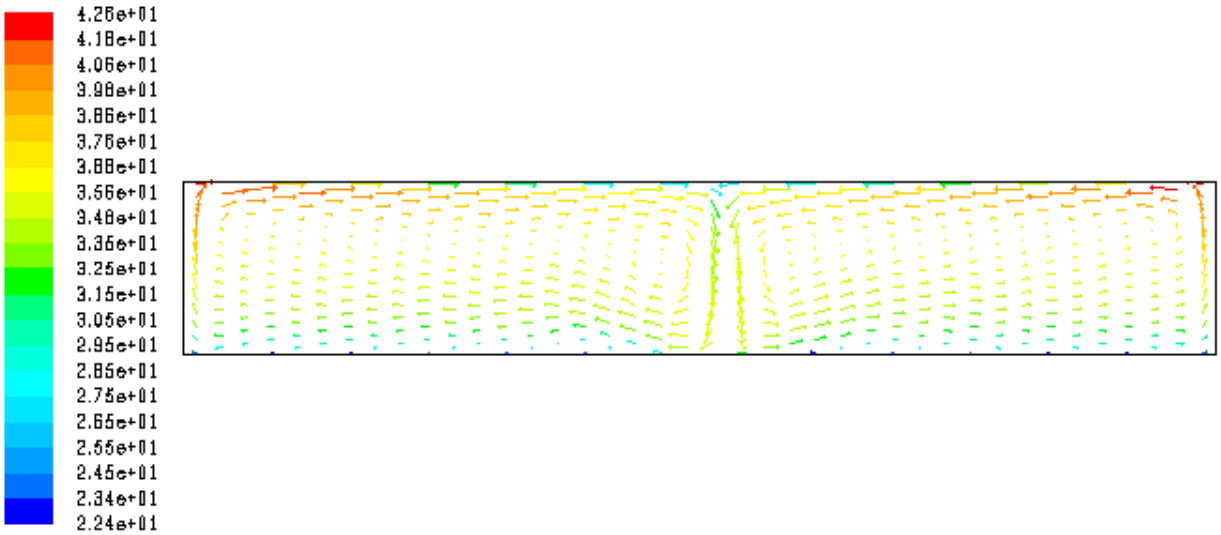

Fig. 6.1. 4 Isotherm of aspect ratio 8

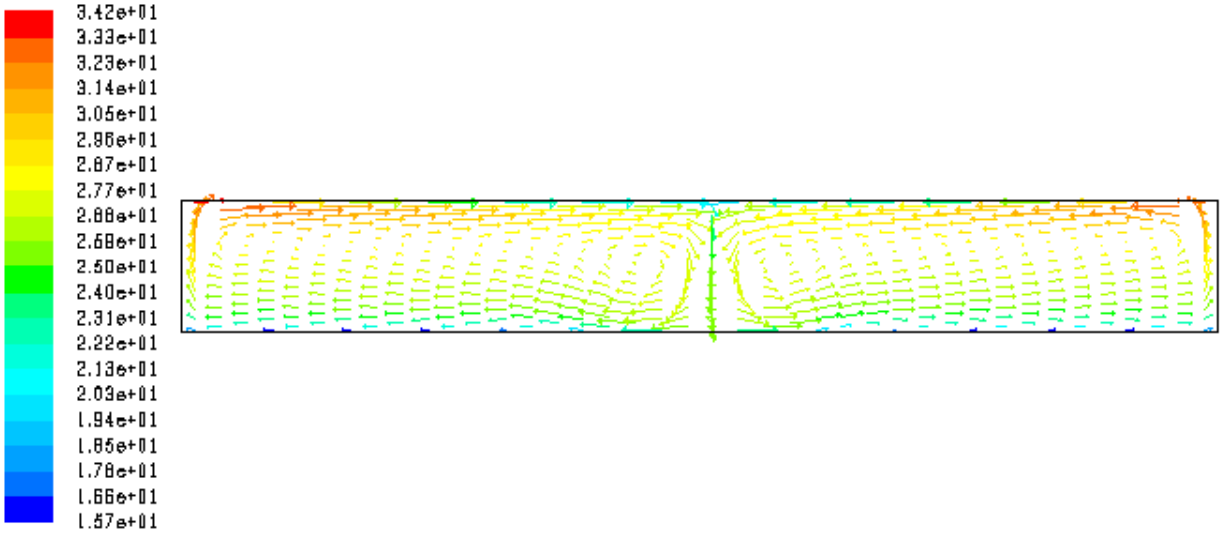

6.2 Contours of Velocity Magnitudes

In 6.2.1 the highest velocity of air particles is 0.456m/s, in 6.2.2 the highest velocity is 0.352m/s, in 6.2.3 the highest velocity is 0.308m/s and in 6.2.4 the highest velocity is 0.303 m/s. In 6.2.1, the highest speed is at the middle – at the mixing region. Vortices are more in 6.2.1 which become parallel as aspect ratio increases. In 6.2.4 are parallel than any other set up in this study and at this point is evident that as aspect ratio increases the flow becomes less turbulent.

Fig. 6.2. 1 Contours of velocity magnitude of aspect ratio 2

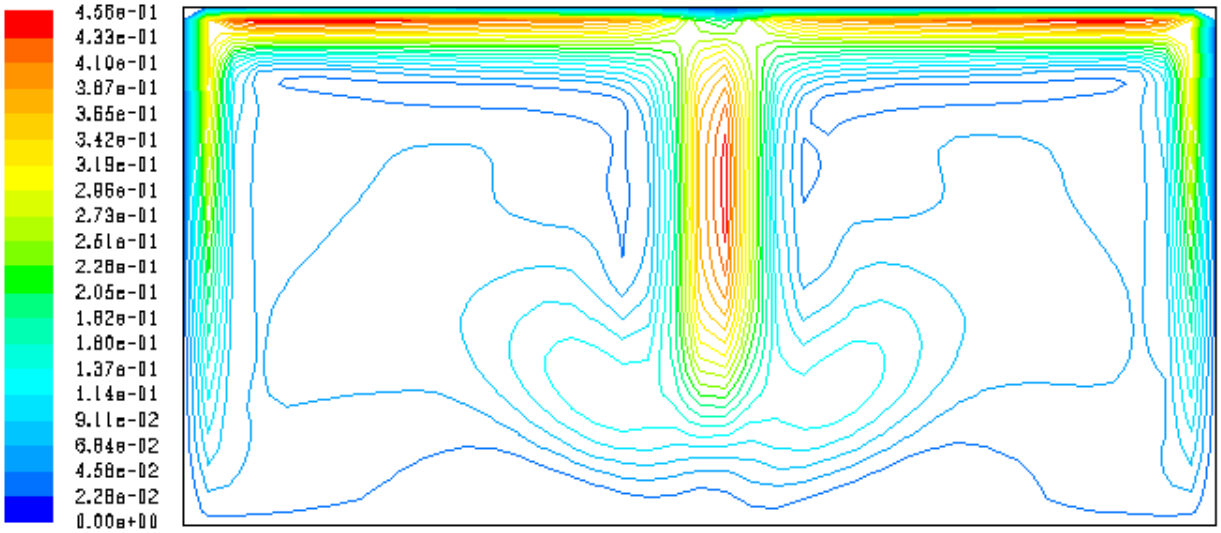

Fig. 6.2. 2 Contours of velocity magnitude of aspect ratio 4

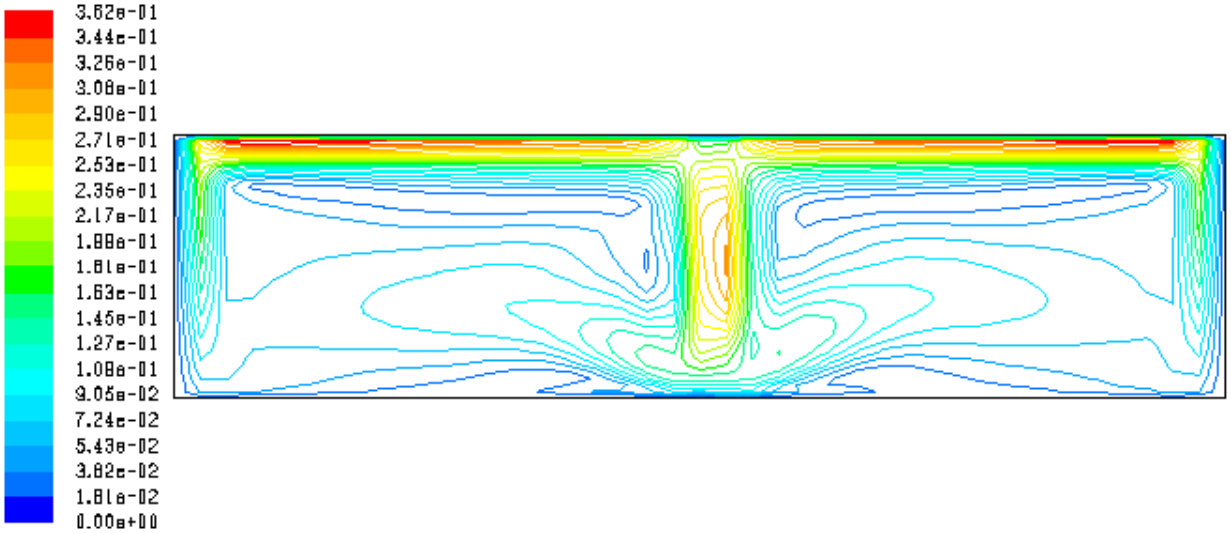

Fig. 6.2. 3 Contours of velocity magnitude of aspect ratio 6

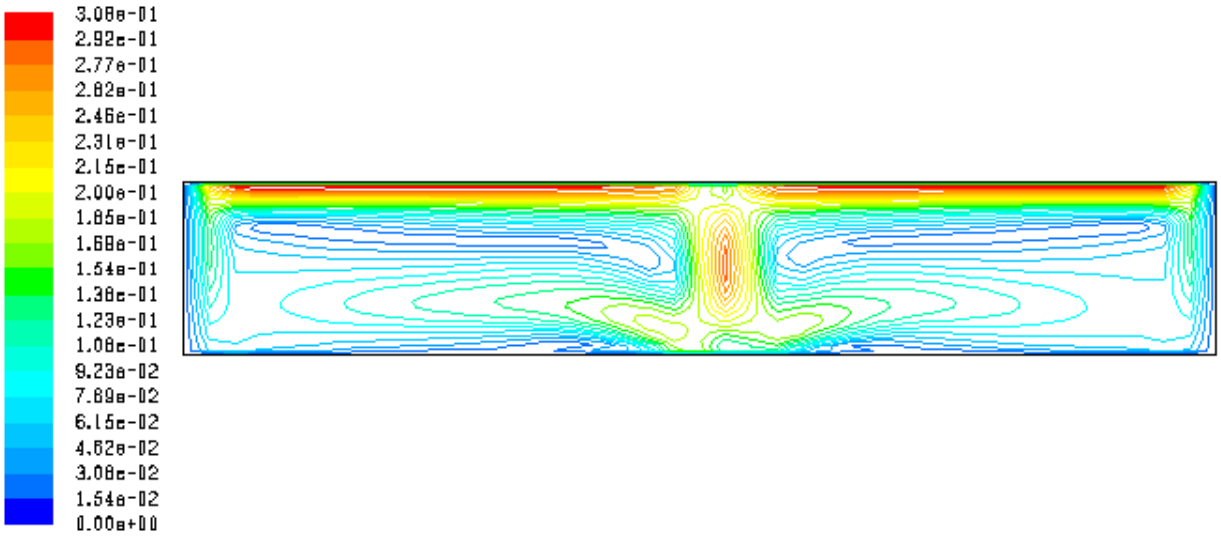

Fig. 6.2. 4 Contours of velocity magnitude of aspect ratio 8

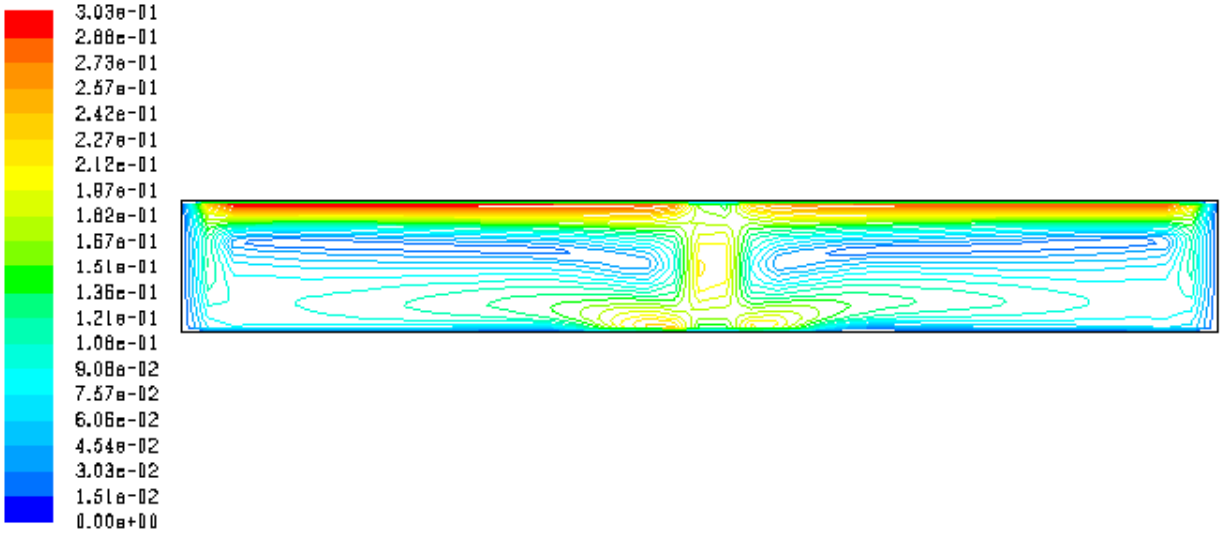

6.3 Streamline Distribution

A streamline is an imaginary line in a fluid such that the tangent at any point shows the path of the speed of a element of the fluid at that point.

The lowest speed of an element indicated here for aspect ratio of 2 is 0.158Kg/s followed by that of aspect ratio 4 which is 0.185Kg/s. This value increases as aspect ratio increases as depicted by that of aspect ratio 6 which is 0.246 Kg/s and the highest speed which is 0.278 Kg/s as shown by that of aspect ratio 8. In 6.3.1, the vortices are big in size and they assume a circular path which deforms as distance increases from their centers. In 6.3.2, radius of centre circle reduces which as well decreases as the aspect ratio increases to 8 as seen in 6.3.3. In 6.3.4 the two centre cell deforms and takes an oval shape. The vortices become parallel as aspect ratio increases.

Fig. 6.3. 1 Contours of streamlines of aspect ratio 2

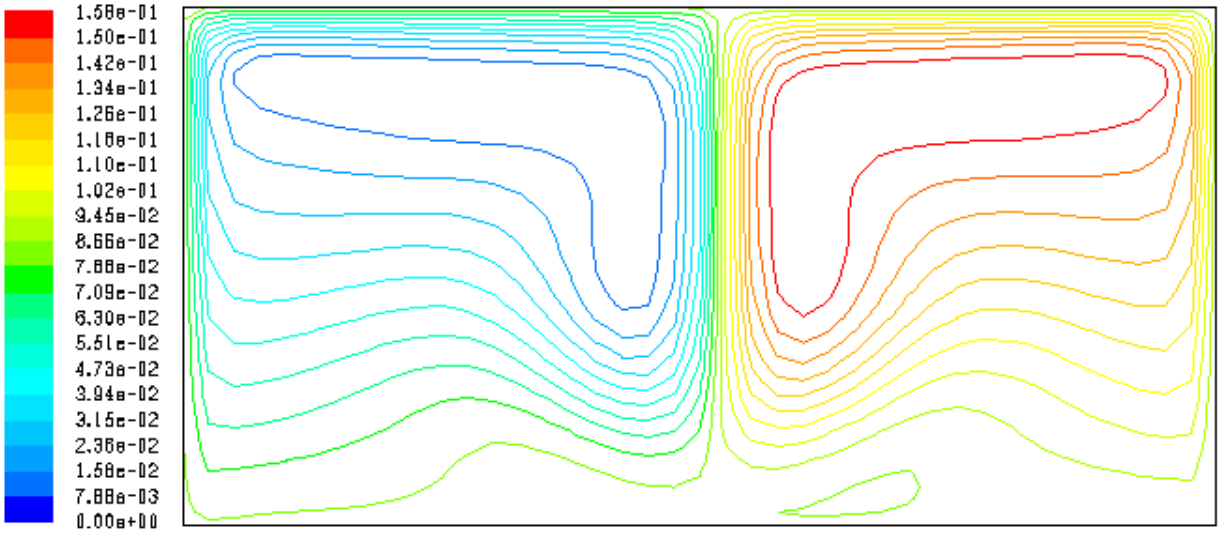

Fig. 6.3. 2 Contours of streamlines of aspect ratio 4

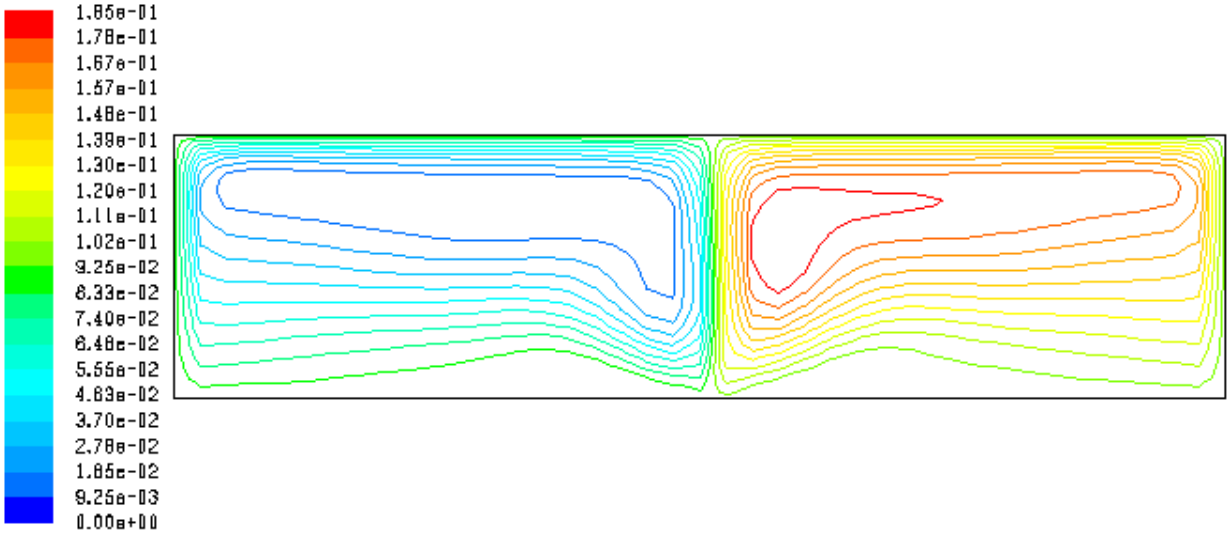

Fig. 6.3. 3 Contours of streamlines of aspect ratio 6

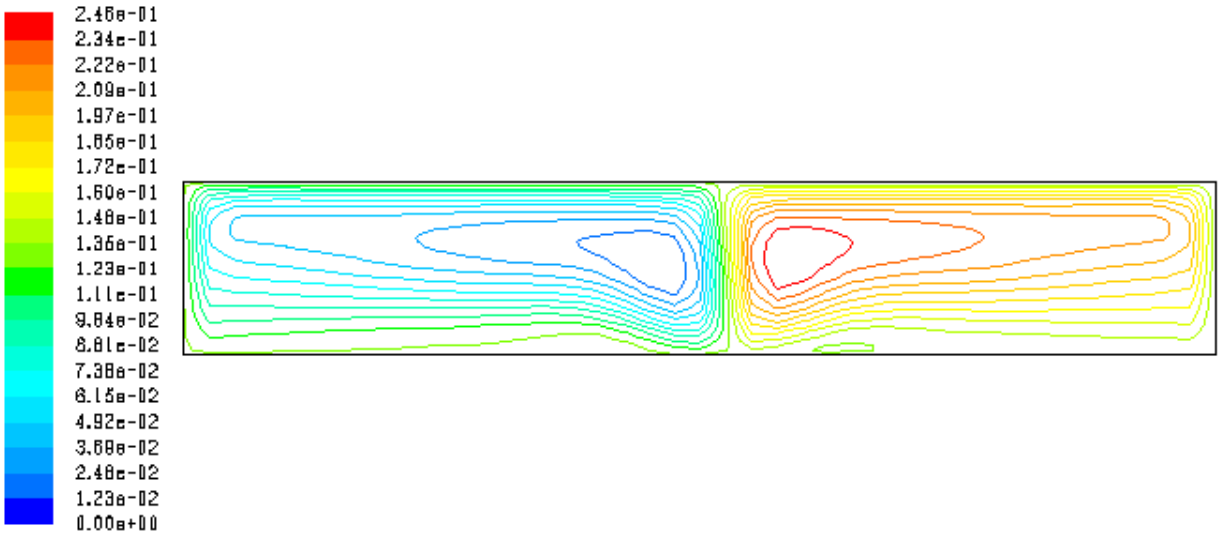

Fig. 6.3. 4 Contours of streamlines of aspect ratio 8

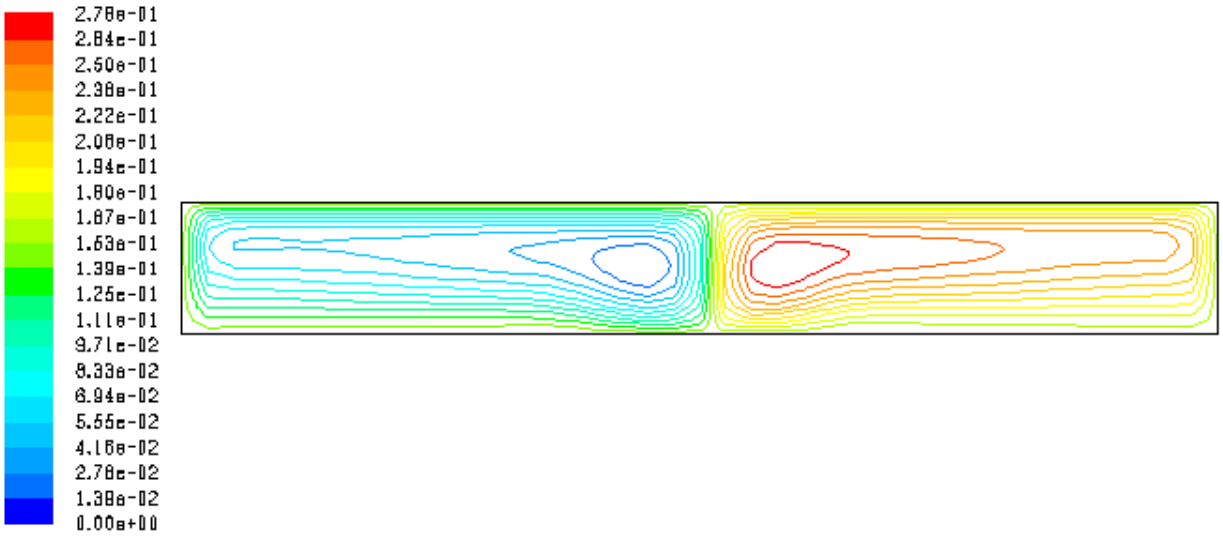

6.4 Conclusion

The objective of the study was to investigate turbulent convection in a rectangular enclosure using SST k-ω model. To achieve this, we had set up specific objectives which were achieved as follows

Numerical data were set for SST k-ω turbulence model. The Boussinesq estimations were utilized, allowing the conservation equations to be simplified. Discretization of governing equations with limit conditions were done using three-point forward and central difference approximations.

Streamlines, isotherms and velocity magnitudes for aspect ratio 2, 4, 6, and 8 were generated and showed that the increase in aspect ratio decreased the turbulence.

The results showed that increased aspect ratio decreased speed and vortices became more parallel thus decreasing turbulence. So, the aspect ratio has an important influence in temperature field and fluid stream in horizontal enclosures heated from the side.

6.5 Recommendations.

Further investigations are recommended for investigating turbulence convection in enclosure by;

i) Using a three-dimensional configuration.

ii) Using same configuration but using Standard k-ω model, Standard $k-\varepsilon$ model, RNG $k-\varepsilon$ model, Realizable $k-\varepsilon$ and RANS model

iii) Varying the characteristics of the fluid contained in the enclosure.

REFERENCES

Aksel, M.H. 2003.*Fluid mechanics*. Ankara: METU Press.

ANSYS (2012), Inc., ANSYS Fluent 14.0 Theory Guide.

Awuor, K. O. (2013). *Simulating Natural Turbulent Convection Fluid Flow in an Enclosure the Two-Equation Turbulent Models* (Doctoral dissertation).

Awuor, K. O., & Gicheru, M. G. M. (2017). Numerical simulation of natural convection in rectangular enclosures. International Journal for Innovative Research in Multidisciplinary Field 3(7) pp. 306-313

Aydin, O.Ünal, A.& Ayhan, T. (1999). Natural convection in rectangular enclosures heated from one side and cooled from the ceiling. *International journal of heat and mass transfer*, *42*(13), 2345-2355.

Ben-Nakhi, A., & Mahmoud, M. A. (2008). Conjugate turbulent natural convection in the roof enclosure of a heavy construction building during winter. *Applied Thermal Engineering*, *28*(11), 1522-1535.

Betts, P. L., & Bokhari, I. H. (2000). Experiments on turbulent natural convection in an enclosed tall cavity. *International Journal of Heat and Fluid Flow*, *21*(6), 675-683.

Bilgen, E. (2002). Natural convection in enclosures with partial partitions. *Renewable Energy*, *26*(2), 257-270.

Bird, R. B., Steward, W. E. and Lightfoot, E. N. (2007), Transport Phenomenon, Wiley & Sons Inc.

Boussinesq, J. (1877). Théorie de l'écoulementtourbillant. *Mem. Présentés par Divers Savants Acad. Sci. Inst. Fr*, *23*(46-50), 6-5.

Braga, E. J. & de Lemos, M. J. (2009). Laminar and turbulent free convection in a composite enclosure. *International Journal of Heat and Mass Transfer*, *52*(3), 588-596.

Chapra, S.C. and Candle, R.P. 1988. *Numerical methods for engineerings*. New York: McGraw-Hill Press.

Chen, S., & Du, R. (2011). Entropy generation of turbulent double-diffusive natural convection in a rectangle cavity. *Energy*, *36*(3), 1721-1734.

Eckert, E. R. G. (1950), Introduction to the Transfer of Heat and Mass,1st Edition.

Faghri, A. Zhang, y. and Howell, J. (2010), Advanced Heat and Mass Transfer, Global Digital Press.

Gatheri, F. K., Reizes, J. A., Leonardi, E., & de Vahl Davis, G. (1994). Natural convection in an enclosure with localized heating and cooling: a numerical study. In *INSTITUTION OF CHEMICAL ENGINEERS SYMPOSIUM SERIES* (Vol. 135, pp. 361-361). HEMSPHERE PUBLISHING CORPORATION.

Goodarzi, M., Safaei, M. R., Oztop, H. F., Karimipour, A., Sadeghinezhad, E., Dahari, M., & Jomhari, N. (2014). Numerical study of entropy generation due to coupled laminar and turbulent mixed convection and thermal radiation in an enclosure filled with a semitransparent medium. *The Scientific World Journal*, *2014*.

Harlow, F. H. and Nakayama, P. I (1968), Transport of Turbulence Energy Decay Rate, Los Alamos Sci. Lab., LA-3854.

Henkes, R. A. W. M., & Hoogendoorn, C. J. (1995). Comparison exercise for computations of turbulent natural convection in enclosures. *Numerical Heat Transfer, Part B Fundamentals*, *28*(1), 59-78.

Hölling, M., &Herwig, H. (2005). Asymptotic analysis of the near-wall region of turbulent natural convection flows. *Journal of Fluid Mechanics*, *541*, 383-397.

Hasanen, M. H., & Akeiber, H. J. (2016). Laminar and Turbulent Natural Convection Simulation with Radiation in Enclosure. In *Applied Mechanics and Materials* (Vol. 818, pp. 3-11). Trans Tech Publications Ltd.

Incropera, DeWitt, Bergman and Levine (2007), Introduction to Heat Transfer, Wiley & Sons Inc., 5th Edition.

Incropera, F.P. and Dewitt, D.P. 2002. *Fundamentals of heat and mass transfer*. New York: John Wiley & Sons Press.

Ingham, D. B. (1978), Free-Convection Boundary Layer on an Isothermal Horizontal Cylinder, Journal of Applied Mathematics and Physics, Vol. 29.

Kays, William, Crawford, Michael, Bernhard and Weigand (2005), Convective Heat and Mass Transfer, McGraw-Hill, 4th Edition.

Krepper, E., Koncar, B. and Egorov, Y. (2006), CFD Modeling of Subcooled Boiling – Concept, Validation and Application to Fuel Assembly Design, Elsevier B.V.

Krepper, E., Rzehak, R. (2011), CFD for Subcooled Flow Boiling: Simulation of DEBORA Experiments, Elsevier B.V.

Kumar, A., Das, D., & Patel, D. (2016) Natural Convection Heat Transfer inside a Narrow Triangular Enclosure with Rectangular Staggered Finned Base Plate: An Empirical Correlation.

Kuznetsov, G. V., &Sheremet, M. A. (2010). Numerical simulation of turbulent natural convection in a rectangular enclosure having finite thickness walls. *International Journal of Heat and Mass Transfer*, *53*(1), 163-177.

Lin, S. J., & Churchill, S. W. (1978). Turbulent free convection from a vertical, isothermal plate. *Numerical Heat Transfer, Part B: Fundamentals*, *1*(1), 129-145.

Mahmoodi, M. (2011). Mixed convection inside nanofluid filled rectangular enclosures with moving bottom wall. *Thermal science*, *15*(3), 889-903.

Markatos, N. C. and Pericleous, K. A. (1984), Laminar and Turbulent Natural Convention in an Enclosed Cavity, International Journal of Heat and Mass Transfer, Vol. 25. pp 755-772.

Martyushev, S. G., & Sheremet, M. A. (2014). Conjugate natural convection combined with surface thermal radiation in a three-dimensional enclosure with a heat source. *International Journal of Heat and Mass Transfer*, *73*, 340-353.

Mobedi, M. 1994. A three dimensional numerical study on natural convection heat transfer from rectangular fins on a horizontal surface. *Ph. D. Thesis Study*.

Oztop, H. F., & Abu-Nada, E. (2008). Numerical study of natural convection in partially heated rectangular enclosures filled with nanofluids. *International Journal of Heat and Fluid Flow*, *29*(5), 1326-1336.

Patankar, S. V. (1980), Numerical Heat Transfer and Fluid Flow, Hemisphere Publishing Co. 1st Edition.

Peng, S. H., & Davidson, L. (2001). Large eddy simulation for turbulent buoyant flow in a confined cavity. *International Journal of Heat and Fluid Flow*, *22*(3), 323-331.

Reynolds, O. (1895), "On the Dynamical Theory of Incompressible Viscous Fluids and the Determination of the Criterion*," Philosophical Transactions of the Royal Society of London*, Series A, Vol. 186, pp. 123.

Reynolds, W. C. (1987). *Fundamentals of turbulence for turbulence modeling and simulation*. STANFORD UNIV CA DEPT OF MECHANICAL ENGINEERING.

Roach, P.J. 1976. *Computational fluid dynamics*. Albuquerque, New Mexico: Hermosa Publishers.

Rodi, W. (1993). *Turbulence models and their application in hydraulics*. CRC Press.

Safaei, M. R., Goshayeshi, H. R., Razavi, B. S., & Goodarzi, M. (2011). Numerical investigation of laminar and turbulent mixed convection in a shallow water-filled enclosure by various turbulence methods. *Scientific Research and Essays*, *6*(22), 4826-4838.

Sharma, A. K., Velusamy, K., Balaji, C., & Venkateshan, S. P. (2007). Conjugate turbulent natural convection with surface radiation in air filled rectangular enclosures. *International Journal of Heat and Mass Transfer*, *50*(3), 625-639.

Sigey, J. K. (2012). *Turbulent natural convection in a rectangular enclosure* (Doctoral dissertation).

Sigey, J. K.Gatheri, F. K., & Kinyanjui, M. (2004).Numerical study of free convection turbulent heat transfer in an enclosure. *Energy Conversion and Management*, *45*(15), 2571-2582.

Tennekes, H; Lumley, J. L. (1972), A First Course in Turbulence, The MIT Press.

Thiault, J. 1985. Comparison of nine three dimensional numerical methods for the solution of the heat diffusion equation. *Numerical Heat Transfer* 8: 281-298.

To, W. M., & Humphrey, J. A. C. (1986). Numerical simulation of buoyant, turbulent flow—I. Free convection along a heated, vertical, flat plate. *International journal of heat and mass transfer*, *29*(4), 573-592.

Tong, L. S. (1965), Boiling heat Transfer and Two-Phase Flow,Wiley& Sons Inc., 2nd Edition.

Walsh, P. C., & Leong, W. H. (2004). Effectiveness of several turbulence models in natural convection. *International Journal of Numerical Methods for Heat & Fluid Flow*, *14*(5), 633-648

Wilcox, M. P. (2013). *Mathematical Modeling of Convective Heat Transfer: From Single Phase to Subcooled Boiling Flows* (Doctoral dissertation, Rensselaer Polytechnic Institute).

Wu, F., Wang, G., & Zhou, W. (2015). A Thermal Non equilibrium Approach to Natural Convection in a Square Enclosure Due to the Partially Cooled Sidewalls of the Enclosure. *Numerical Heat Transfer, Part A: Applications*, *67*(7), 771-790.

Wu, F., Zhou, W., & Ma, X. (2015). Natural convection in a porous rectangular enclosure with sinusoidal temperature distributions on both side walls using a thermal non-equilibrium model. *International Journal of Heat and Mass Transfer*, *85*, 756-771.

Xamán, J., Arce, J., Álvarez, G., & Chávez, Y. (2008). Laminar and turbulent natural convection combined with surface thermal radiation in a square cavity with a glass wall. *International Journal of Thermal Sciences*, *47*(12), 1630-1638.

Yeoh, G. H. and Tu, J. Y. (2009), Modelling Subcooled Boiling Flows, Nova Science Publishers, Inc.

Zdanski, P. S., VazJr, M., & Gargioni, G. T. (2016). Convection heat transfer enhancement on recirculating flows in a backward facing step: the effects of a small square turbulence promoter. *Heat Transfer Engineering*, *37*(2), 162-171.